

MOLECULAR DYNAMICS SIMULATION AND ITS APPLICATION TO NANO-RHEOLOGY

Ahmad Jabbarzadeh and Roger I. Tanner

School of Aerospace, Mechanical and Mechatronic Engineering,
The University of Sydney, NSW 2006, Australia

ABSTRACT

Over the last 15 years molecular dynamics (MD) simulations have become one of the important tools to tackle many of the complex problems that are faced by rheologists and engineers. The advent of modern areas of science such as nano-technology and the need to understand physical phenomena including rheology and tribology at the molecular scale have helped the growth of research both experimentally and computationally at nano-scales. Molecular dynamics simulations among other molecular simulation methods have been used for computational research in those areas. Application of molecular dynamics to rheology has helped to understand the behaviour of polymers qualitatively; also important progress has been made in predicting quantitative rheological properties such as the viscosity of simpler liquids (such as alkanes). In particular the application of MD to the behaviour of confined fluids and lubricants at nano-scales has revealed some important properties and explained the underlying physics of observed phenomena that include enhanced viscosity and relaxation times and the role of normal stress differences in supporting large loads. MD has been a valuable tool in studying the relationship of the molecular structure and the rheological properties. In this review we will give an introduction about the method and will discuss some of the progress made to date. Our main focus will be on the application of MD in the nano-rheology of ultra-thin confined films.

KEYWORDS: Rheology; molecular dynamics simulation; nano-rheology; confined films; boundary conditions; slip; friction; tribology; polymers, liquid crystals, amorphous surface, crystalline surface.

1. INTRODUCTION

The idea of using molecular dynamics for understanding physical phenomena goes back centuries. About 180 years ago, long before the availability of computers, Laplace beautifully described the idea as “Given for one instant an intelligence which could comprehend all the forces by which nature is animated and the respective situation of the beings who compose it - an intelligence sufficiently vast to submit these data to analysis - it would embrace in the same formula the movements of the greatest bodies of the universe and those of the lightest atoms, nothing would be

uncertain and the future, as the past, would be present to its eyes.” [1]. We call this collection of bodies a *system*. In order to predict the movements of the parts of a system we need to know the forces acting between them and we also need an intelligence that can analyse the data. For the first requirement we have to devise a model that mimics the real physical forces between the bodies. Availability of fast-computing machines has brought Laplace’s dream to reality by providing a vast “intelligence” for analysing data. In recent years the application of molecular dynamics (MD) to important problems in material science in general and rheology in particular has made it an indispensable analysis tool that sheds light on places and problems that are hardly accessible by other methods. Physical models and reductionism are born out of the necessity to explain the world in simple terms and predict the behaviour and properties of physical systems through our limited sources for data processing. As we gain more powerful data processing tools reductionism becomes less important and we can tackle problems from first principles. We have come a long way in the past decades in expanding the size and complexity of the systems that are studied by MD simulations. Perhaps in future with utilization of new techniques such as quantum computations we will be able to tap even further into the power that was envisaged by Laplace.

In the usual situations where continuum mechanics can be used for calculation of macroscopic properties, MD is an inefficient way of doing those calculations. However there are circumstances in which the fluid under analysis does not follow continuum models, or there is no such a model to describe the behaviour of fluid. An example of these situations is in highly confined fluids where the inhomogeneity induced by the confining surface renders continuum equations useless or irrelevant; in other situations the boundary condition is not known. Also when one is interested in molecular scale dynamics and processes that involve molecular level time scales, molecular dynamics simulations should be considered. One of the promising areas in this field is to investigate the molecular structure and its effect on the overall behaviour of the fluid and its mechanical properties. Thus one could design molecules that yield desired properties for the fluid of interest. This could be a polymer melt, lubricant or a drug delivery agent. These capabilities make MD an indispensable tool in the currently flourishing area of nano-technology. The information obtained by MD in some cases is very hard to obtain by any other methods either because of the lack of experimental techniques or working models. In this review we will discuss the basic technical methods involved in typical MD calculations. Interested readers can find more detailed discussions of the technical details from the works by Haile [2], Allen and Tildesley [3] and Rapaport [4].

Unlike Newtonian fluids, polymer melts and other types of materials that behave in a non-Newtonian manner lack a universally agreed constitutive equation to model their behaviour. This has led researchers to look in other directions including MD. Two aspects of molecular dynamics that have made it a valuable tool are the study of polymer rheology in general and nano-rheology in particular for systems in equilibrium and far from equilibrium. While the fundamental analysis of the system in equilibrium studies the static properties of the material, non-equilibrium molecular dynamics (NEMD) studies transport phenomena and dynamic properties. Unlike

equilibrium molecular dynamics, NEMD is a fairly new development. [5]. This method initially was used to study the rheology of simple Lennard-Jones soft spheres, however more complex molecules, such as short chain and branched molecules are now widely being simulated using this method. Thus simulations of chains with a few hundreds or thousands of monomers are not uncommon. For a rheologist calculation of viscosity and normal stresses are of great interest. The NEMD method allows the calculation of the shear viscosity; but other dynamic properties of individual molecules of interest can also be found. One of the interesting outcomes of these simulations captures the shear thinning or non-Newtonian behaviour where the viscosity decreases with shear rate. This phenomenon is widely known for polymer melts. However, the simulations have shown, even for simple fluids that are Newtonian at lower shear rates (they are Newtonian only on the time scales of common observations) that they act in a non-Newtonian way at higher shear rates; the critical shear rate at which the transition to a non-Newtonian regime begins is the inverse of the relaxation time of the molecules in the system. In order to get a good signal to noise ratio, the shear rates examined in NEMD are usually larger than 10^7 s^{-1} ; that is, at least 2-3 orders of magnitude larger than what is typically achievable by rheometers and experimental techniques in the laboratory. However, the gap between what is accessible by experiments and NEMD does not prevent us drawing important conclusions, and making an analogy between the behaviour of simple fluids being simulated at large shear rates and those being measured in the laboratory. The high shear rates simulated by NEMD are actually encountered in some physical situations. For example the shear rates experienced by a lubricant layer on a hard disk in a computer could be as high as 10^9 - 10^{10} s^{-1} . In those situations the application of NEMD is the only way to examine the properties of the liquid film. One of the achievements of NEMD has been to explain the molecular origin of many rheological observations such as shear thinning; the orientation of molecules in the flow direction makes the flow in that direction much easier and so naturally we encounter a lower viscosity or shear thinning. The rheology of bulk materials is usually estimated by use of NEMD algorithms such as SLLOD [5] and Green-Kubo [5, 6] methods. Most of the existing NEMD simulations have been done either for Couette planar shear or Poiseuille flows although limited attention has also been given to develop algorithms for extensional flows by Matin et al. [7]. The boundary driven methods that we mainly discuss here are usually used in the study of boundary lubricant rheology or the rheology of confined fluid. That area usually is called nano-rheology and has significant applications in materials science in general and nano-technology in particular. This will include work done on the simulation of fluid properties in nano-pores and confined geometries, thin lubricant film rheology, boundary conditions and slip analysis and structural design of liquids at the molecular level.

1.1 Theory and Simulation

On the molecular scale, in a system of particles that represents a form of matter in its gaseous, liquid or solid form, the state of the system can be described by the positions and momenta of the molecules. However on a macroscopic scale we prefer to describe the state of the system by a set of observable quantities like temperature, pressure, etc. Physical theories often try to establish a relationship between these

macroscopic observable quantities. In molecular scale simulations it is kinetic theory and statistical mechanics that take the role of compiler for interpreting the connection of the raw data, which are the velocities and positions of molecules, to the macroscopic observable quantities. Rather than trying to obtain a simplified closed form expression to describe the behaviour of the system (theory), molecular scale simulations proceed by first principles and directly simulate the original system. Then the results of the simulation can be openly inspected for behaviour, and for possible explanations of such a response.

1.2 Molecular scale simulations

The earliest work in molecular scale simulation was accomplished by Metropolis *et al* [8]. This work was fundamental for the so-called Monte Carlo (MC) method. Early models were for idealised hard spheres (three dimensional) and hard disks (two dimensional). Later on the MC method was successfully used with a Lennard-Jones potential for soft spheres [9]. The first molecular dynamics simulation by Alder and Wainwright [10] on hard spheres opened the way for MD simulations. Later Rahman [11] conducted an MD simulation for soft spheres with Lennard-Jones potentials. The work on the Lennard-Jones model was followed by other researches through the years. These simulations further flourished with the simulation of diatomic molecular liquids [12], followed by an MD simulation for liquid water [13]. Later, work on rigid molecules [14] and flexible molecules of liquid n-butane [15] and proteins [16] paved the way for more complex systems of molecules. Since then there have been numerous simulations in various applications for understanding physical phenomena through molecular dynamics simulation.

Molecular simulations have passed the limitations of equilibrium computations and are now being used for finding transport coefficients by means of the so-called non-equilibrium molecular dynamics (NEMD) method [17-20]. Isothermal and isobaric algorithms have been devised for NEMD [21-23]. The rheological properties of homogenous LJ fluids [24, 25], and diatomic liquids [26] and polymeric liquids and dilute solutions [27-29] and alkanes [30-33] have all been studied through NEMD.

Molecular scale simulations are usually accomplished in three stages by developing a molecular model, calculating the molecular positions, velocities and trajectories, and finally collecting the desired properties from the molecular trajectories. It is the second stage of this process that characterises the simulation method. For molecular dynamics (MD) the molecular positions are deterministically generated from the Newtonian equations of motion. In other methods, for instance the Monte Carlo method, the molecular positions are generated randomly by stochastic methods. Some methods have a combination of deterministic and stochastic features. It is the degree of this determinism that distinguishes between different simulation methods. Although the present review is restricted to molecular dynamics and especially non-equilibrium molecular dynamics (NEMD) in rheology, it should not be forgotten that other “molecular” methods, such as Brownian dynamics, are available for the study of polymer solutions and long polymer chains. The Monte Carlo method [8] and various particle dynamics methods are also of interest in rheology. However

any attempt to include these methods in this review has had to be resisted because of space limitations.

2. MOLECULAR DYNAMICS SIMULATION TECHNIQUES

We begin with a brief description of the techniques. Readers already well versed in the field may go directly to Section 3. In a molecular dynamics simulation a number of molecules are put in a simulation box and the position and velocity of these particles are calculated at small time intervals by integrating the equations of motion that govern the motion of particles through the phase space. The integration schemes are based on simple finite difference methods. Traditionally different versions of Verlet's algorithm [34] or Gear's predictor-corrector algorithm [35, 36] are used depending on various considerations in the problem and the required level of accuracy. Periodic boundaries are often used in the required directions to mimic an infinite system. Usually the force computation is the most time consuming part of any molecular dynamics algorithm. This huge computational task can however be reduced by incorporating some techniques such as the Verlet neighbour list and link-cells methods. The analyses of the generated data are done through kinetic theory and statistical mechanics. The accuracy of the calculated time average properties should also be tested through the usual statistical methods to make sure that the obtained properties are reliable within specified statistical uncertainties.

2.1 Molecular models and potentials

The most common model that describes matter in its different forms is a collection of spheres that we call "atoms" for brevity. These "atoms" can be a single atom such as Carbon (C) or Hydrogen (H) or they can represent a group of atoms such as CH₂ or CS₂. These spheres can be connected together to form larger molecules. The interactions between these atoms are governed by a force potential that maintains the integrity of the matter and prevents the atoms from collapsing. The most commonly used potential, that was first used for liquid argon [38], is the Lennard-Jones potential [39]. This potential has the following general form:

$$\phi_{LJ}(r) = A\epsilon \left[\left(\frac{\sigma}{r_{ij}} \right)^m - \left(\frac{\sigma}{r_{ij}} \right)^n \right], \quad \text{.....(1)}$$

where $r_{ij} = r_i - r_j$ is the distance between a pair of atoms i and j . This potential has a short range repulsive force that prevents the atoms from collapsing into each other and also a longer range attractive tail that prevents the disintegration of the atomic system. Parameters m and n determine the range and the strength of the attractive and repulsive forces applied by the potential where normally m is larger than n . The common values used for these parameters are $m = 12$ and $n = 6$. The constant A depends on m and n and with the mentioned values, it will be $A = 4$. The result is the well-known 6-12 Lennard-Jones potential. Two other terms in the potential, namely ϵ and σ , are the energy and length parameters. The energy parameter ϵ , sometimes referred as well-

Quantity	Unit	Quantity	Unit
Length:	σ	Velocity:	$(\epsilon/m)^{1/2}$
Mass:	m	Density:	σ^3
Energy:	ϵ	Stress:	ϵ/σ^3
Shear rate:	$(\epsilon/m\sigma^2)^{1/2}$	Viscosity:	$(m\epsilon)^{1/2}/\sigma^2$
Temperature:	ϵ/k_B	Stiffness:	$\epsilon\sigma^2$
Time:	$(m\sigma^2/\epsilon)^{1/2}$	Normal Stress Coefficient:	m/σ

Table 1: Lennard-Jones reduced units. σ , m and ϵ are molecular diameter, mass and energy parameter respectively.

depth, is the minimum energy for ϕ . The length parameter σ is the distance between two interacting atoms when the potential energy is zero. σ is sometimes referred to as the atomic or molecular diameter, though this description may not be quite true for atoms that are treated as soft spheres. Nevertheless it gives an idea of the dimension of the atoms. The energy and length parameters depend on the type of the atoms involved in the pair interaction. For example $\sigma = 0.393$ nm and $\epsilon/k_B = 47$ K are used for united atom representations of ethyl (CH_2) groups. To minimize the extremely large or small numbers in the simulations the computations are often conducted under reduced units conventions where the mass, energy (ϵ) and size (σ) of the suitably chosen atom are used as units for mass, energy and length. All the properties that are calculated will naturally have reduced dimensions. The reduced units are given in table 1 for various properties. After the computations the values can be converted to suitable SI units.

For a system of N atoms, taking into account all pair interactions results in $N(N-1)/2$ interactions, a number that can be very large even for moderate numbers of atoms. However since the potential vanishes at large distances it is often assumed that it can be truncated beyond a certain distance r_c which is called the cut-off radius. The potential then can be shifted so that it goes smoothly to zero at $r = r_c$. This strategy significantly reduces the number of interactions. The truncated shifted form of the Lennard-Jones potential is:

$$\phi_{LJ}(r) = \begin{cases} 4\epsilon \left[\left(\frac{\sigma}{r} \right)^{12} - \left(\frac{\sigma}{r} \right)^6 \right] - \phi_{shift}, & r \leq r_c \\ 0, & r \geq r_c \end{cases}, \quad \dots\dots\dots(2)$$

where:

$$\phi_{shift} = 4\epsilon \left[\left(\frac{\sigma}{r_c} \right)^{12} - \left(\frac{\sigma}{r_c} \right)^6 \right].$$

The force between two interacting atoms then can be found by differentiating the force potential $f = -d\phi/dr$. It is suggested that the choice of cut-off especially near the critical point can affect the phase diagram and thermodynamic properties [37]. Choices of $r_c = 2^{1/6}\sigma$ (pure repulsive force) or $r_c = 2.5\sigma$ have been widely used in the literature. However, long-range corrections are made to some of the properties like pressure and total energy at the end or during the simulation. For constant volume simulations a constant value must be added to the final results for some properties [3]. For constant pressure simulations the correction should be done during the simulations.

In the case of a molecular system several interaction sites or atoms are connected together to form a long chain, ring or a molecule in other forms. In this case, in addition to the mentioned Lennard-Jones potential, which governs the intermolecular potential, other potentials should be employed. An example of an intramolecular potential is the torsional potential, which was first introduced by Ryckaert and Bellemans [15] in the simulation of n-butane for the torsional motion of the atoms about the bonds of the same molecules. Bonds that keep the atoms in the structure of a molecule are often modelled as rigid rod connectors. They can also be modelled as a stiff spring with a potential similar to that of a linear Hookean spring. Other molecular models are also commonly used such as SHAKE and RATTLE models where the bond length or bond angles are fixed during the simulations. These semi-rigid molecules are however more difficult to simulate and due to the special algorithm the time steps used are usually smaller.

For simulation of real fluids in order to obtain meaningful physical quantitative results the values for ϵ and σ should be determined carefully. This is done by series of simulations to get physical properties close to those determined by experiments for the material that is being simulated. For simulation of real molecular fluids the choice of the simulation parameters is more complex as one should also choose proper values for the intramolecular potential as well. As examples of real fluids that have been widely simulated by researchers liquid argon (atomic fluid) and various alkanes (molecular fluid) can be named. Generic simulations in terms of reduced units are also widely used for obtaining qualitative results.

The movement of the atoms in the atomic system is governed by Newtonian dynamics given by:

$$\mathbf{F}_i = m_i \ddot{\mathbf{r}}_i \quad \text{.....(3)}$$

where m is the mass of the atom. Equation (3) gives the equations of motion for the N-body system. However these equations can be written in various forms. The most common form is to write the equations in terms of the momenta and positions. These are given by:

$$\frac{\mathbf{p}_i}{m} = \dot{\mathbf{r}}_i \quad , \quad \text{.....(4)}$$

$$\dot{\mathbf{p}}_i = \mathbf{F}_i \quad , \quad \text{.....(5)}$$

where \mathbf{p} and \mathbf{r} are the momentum and position. Equations (4) and (5) are well known equations of motion that give the positions and momenta of the atoms. Using these two equations any system of N particles can be represented by $6N$ first order differential equations, which is equivalent to $3N$ second order differential equations given by equation (3). These equations can be solved by finite difference methods. There are many methods available for solving sets of first order differential equations. In any molecular dynamics algorithm force computation is the most time consuming part. Thus any chosen finite difference method should do the integration with minimum need for the force computation. Popular finite difference schemes such as Runge-Kutta are rarely used in molecular dynamics [2]. Historically two finite difference methods have been used in most of the MD simulations. These two methods are the Verlet algorithm [34] and the Gear predictor-corrector algorithm [36]. The Gear algorithm is of higher order compared to the Verlet algorithm, so it offers a higher level of accuracy. However, comparing the energy conservation properties at large time steps the Gear algorithm lags behind the Verlet algorithm. This makes Verlet more attractive for its ability to use larger time steps; however this might be associated with some loss in accuracy. In the final averaged results both methods basically give the same statistical uncertainties. So for most of the simulations it is a matter of personal taste which integration method is chosen.

2.2 Imposing boundary conditions

In MD simulations the way the molecules or atoms interact with their surroundings must be implemented in a proper way. In general the boundaries of the simulation region can be one of the following three possibilities:

1. Periodic boundaries.
2. Sliding periodic boundaries.
3. Hard boundaries.

The periodic boundaries are applied in the directions where one intends to simulate an infinite system. The periodicity is applied by introducing a *primary cell* surrounded by its *images* in the periodic directions. Figure 1 shows a two dimensional view of the primary cell surrounded by its replicas. Whenever a particle exits from one face of the primary cell another image particle enters from the opposite face. The number of the particles in the primary cell remains constant and the particles in the small volume of the simulation box will represent the macroscopic system fairly well. In general only the information about the atoms in the primary cell needs to be stored. The interaction between the particles is governed by the minimum image convention where each particle interacts with the closest periodic image of the other particles including the one in the same cell. Some modifications should be applied to make the

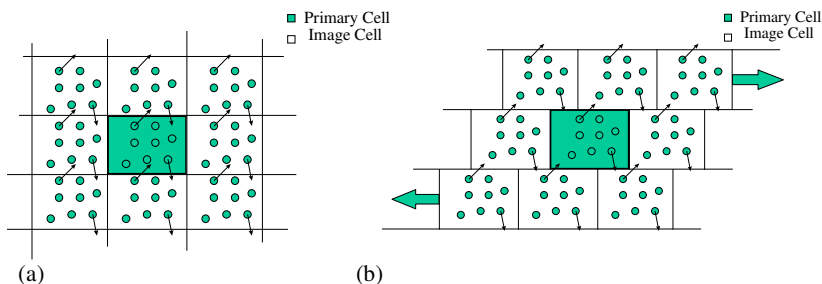


Figure 1: (a) Periodic boundaries shown for two dimensions. The cell in the centre is the primary cell surrounded by its replicas. (b) Sliding periodic boundaries in two dimensions. This kind of periodic boundaries is used in NEMD simulation of homogenous shear flow.

periodicity applicable to homogenous shear flow. Usually to apply a flow field a boundary driven method (moving hard boundaries) can be used. However this results in undesirable effects due to presence of the wall that induces inhomogeneity. To avoid this, and to measure the properties of a homogenous system (bulk properties); the sliding periodic boundaries method [17] is used. This so called non-equilibrium molecular dynamics (NEMD) method is widely used for the simulation of bulk homogenous fluids. Figure 1 shows the sliding periodic boundaries method in two dimensions. In this method the upper and lower layers are moving relative to the primary cell with a velocity proportional to their distance from the primary cell in the direction normal to the flow. This method induces a uniform shear rate across the flow. Whenever a particle leaves the primary cell its position and velocity should be adjusted according to the velocity gradient. Hard boundaries are used in the study of the surfaces or solid-fluid interfaces. Also they are used to induce a boundary driven flow. In this case also, periodic boundaries are usually applied in the directions that extend to infinity. The solid boundaries may be in the form of hard reflecting walls or structured atomic walls with a potential that keeps the fluid particles inside the simulation box. Although a hard reflecting wall, represented by a simple potential, is less expensive computationally, atomic representation of the wall is closer to physical reality.

2.3 Economising the computational effort

As mentioned before the force computation from pair interactions is the most time consuming part in the MD simulations. Of course, use of Newton's third law can halve the number of calculations. But using all the pair interactions can still be very wasteful when the size of the simulation box is much larger than the cut-off distance.

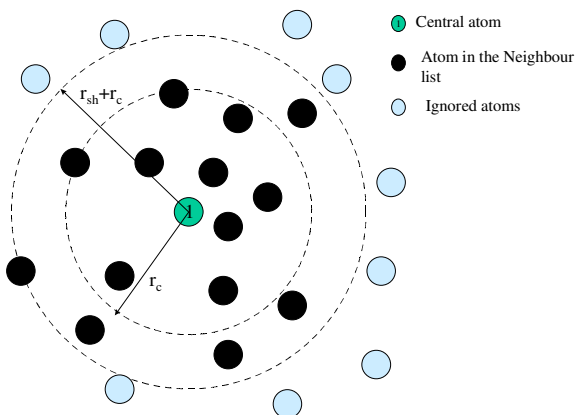


Figure 2: This schematic view shows how the neighbour list method is implemented for atom 1 in the centre. Here r_c is the cut off radius and r_{sh} is the neighbour list shell. Only atoms in the range of $(r_c + r_{sh})$ are put in the interaction list.

Since the Lennard-Jones potential mentioned in Section 2.1 is a short range potential some techniques can be used to improve the computational efficiency. Two techniques are commonly used in MD simulations. They are the Verlet neighbour list method [34] and the link-cells method [40]. A brief description of these methods will be given here.

Because of the small time steps used in the simulation the microscopic configuration of the atoms changes very slowly over the time. So a list of neighbouring atoms, which are in the interaction range, will remain valid over many time steps. This will save time on rechecking all the atoms in the system. To apply the method successfully and to make it stay valid for longer times a neighbour list shell (r_{sh}) is defined. Figure 2 shows a schematic view of the molecules. In making a neighbour list for the central molecule 1 only those molecules are put in the list which are within a distance $r_c + r_{sh}$ from the molecule 1. The neighbour list typically is updated every 10-20 time steps through monitoring the maximum velocity in the system and refreshing the list when the following condition is satisfied:

$$\sum_t v_{i,\max} > \frac{r_{sh}}{2\delta t} \quad \text{.....(6)}$$

where $v_{i,\max}$ is the maximum velocity of the particles in the system at a given time step [4].

The Link-Cells method is used when the size of the simulation box is many times larger than the cut off radius r_c . Consider a rectangular volume as the simulation

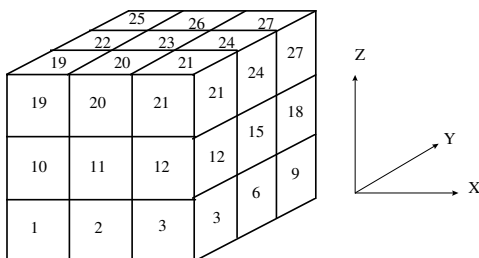


Figure 3: A three dimensional implementation of the link-cells method. For an atom in cell number 14 (in the centre of the cube), only cells 14,15,16,17,18,19,20,21,22,23,24,25,26 and 27, need to be searched for potential interaction candidates.

box. This volume can be divided into small cells where the side of each cell is slightly larger than the cut off radius r_c . Then any atom in a given cell can possibly interact with the atoms either in the same cell or in the immediately neighbouring cells. This can be illustrated with a three dimensional example shown in Figure 3. Consider that the simulation box is divided into $3 \times 3 \times 3$ cells. For cell number 14, which is located in the centre, there are 26 neighbouring cells in three directions. For an atom in the cell 14 only half the neighbouring cells and the cell 14 itself (total of 14 cells) need to be searched for the potential interaction partners. This means any part of the cells will be searched only once in the process of building the pair interaction list. So for example interaction between cells 14 and 13 will be checked when cell 13 is the centre of attention. This makes it possible to take the most advantage of Newton's third law. As a result, in tabulation of the pair interactions, only one interaction between atoms i and j will be recorded. This avoids double counting of the interactions and also improves the computational efficiency of the algorithm. The search through the neighbouring cells is more efficient than checking all pairs in the system. It reduces the computational effort from $O(N^2)$ to $O(N)$ where N is the number of atoms in the system [4].

2.4 Calculating macroscopic properties

To derive useful information from the detailed microscopic behaviour of the system, it is necessary to relate the microscopic information to the macroscopic properties. This task is achieved by using statistical mechanics. Thermodynamic state properties such as temperature, pressure and internal energy as well as other quantities such as the stress tensor and viscosity can be calculated by using relevant equations of state. Other structural properties of interest can be also calculated from the microscopic position of the particles in the system. At any given time a system of N particles can be described by a point in a $6N$ dimensional *phase space* Γ . Phase space has two components, a $3N$ dimensional *configuration space* and a $3N$ dimensional

momentum space. The path through which the point in phase space evolves with time is called the phase space trajectory. So at a given time t the positions and momenta of all particles in the system correspond to a single point on the phase space trajectory. All the other properties computed in a MD simulation are a function of phase space. So these properties also evolve with time as the system passes along the phase space trajectory. For some property such as $A(\Gamma(t))$ which is a function of the phase space the instantaneous value is not a constant with respect to time. A is a fluctuating quantity with time and any measurement for this property should be done during a long enough period of time. So the time average for A will be:

$$\langle A \rangle = \lim_{t \rightarrow \infty} \frac{1}{t} \int_0^t A(\Gamma(t)) dt \quad \dots\dots\dots(7)$$

where angled brackets denote the time average.

2.4.1 Stress tensor

For a rheologist it is important to relate the microscopic state of the system to the stress tensor. The microscopic derivation of the stress tensor is due to Irving and Kirkwood [41] and can be also found in [5]. Without going into details of the derivation, the expression for the instantaneous stress tensor is (note we use the tensile stress is positive convention, as do most rheologists; some authors use the pressure tensor (compression positive))

$$\sigma(\mathbf{r}, t) = -\frac{1}{V} \sum_i \left[m_i (\mathbf{v}_i(t) - \mathbf{U}(\mathbf{r}_i, t)) (\mathbf{v}_i(t) - \mathbf{U}(\mathbf{r}_i, t)) + \sum_{j>i} \mathbf{r}_{ij}(t) O_{ij}(t) \mathbf{F}_{ij}(t) \right] \Big|_{\mathbf{r}_i(t)=\mathbf{r}} \quad \dots\dots\dots(8)$$

In equation (8) the first term in the summation is the kinetic contribution to the stress tensor where m_i is the mass of particle i , \mathbf{U} is the streaming flow velocity, V is the total volume of the system and \mathbf{v}_i is the velocity of particle i . The second term represents the contribution of the potential to the stress tensor where $\mathbf{r}_{ij} = \mathbf{r}_i - \mathbf{r}_j$ is the distance vector between particle i and j and \mathbf{F}_{ij} is the force on particle i due to particle j . O_{ij} is a differential operator which is given by:

$$O_{ij} = 1 - \frac{1}{2} \mathbf{r}_{ij} \cdot \frac{\partial}{\partial \mathbf{r}} + \dots + \frac{1}{n!} \left[-\mathbf{r}_{ij} \cdot \frac{\partial}{\partial \mathbf{r}} \right]^{n-1} + \dots \quad \dots\dots\dots(9)$$

For bulk fluids with pair-wise interactions $O_{ij} = 1$. For inhomogeneous fluids if the intention is to calculate the average stress tensor across a channel, $O_{ij} = 1$ can be used as a reasonable approximation and has been proved [42] to give consistent results. However if one studies the local stress tensor across a channel within an inhomogeneous fluid a better method can be used, such as the *method of planes* [43]. The approximate value $O_{ij} = 1$ is often used and this yields the expression for the time average stress tensor as:

$$\boldsymbol{\sigma} = -\frac{1}{V} \left\langle \sum_i \left[m_i (\mathbf{v}_i - \mathbf{U}(\mathbf{r}_i)) (\mathbf{v}_i - \mathbf{U}(\mathbf{r}_i)) + \sum_{i,j} \mathbf{r}_{ij} \mathbf{F}_{ij} \right] \right\rangle. \quad \text{.....(10)}$$

2.4.2 Kinetic temperature

Each translational degree of freedom in the system contributes $k_B T/2$ to the kinetic energy so that the instantaneous kinetic temperature will be:

$$T(t) = \frac{1}{(3N - C)k_B} \sum_{i=1}^N \left[m_i (\mathbf{v}_i(t) - \mathbf{U}(\mathbf{r}_i, t))^2 \right] \quad \text{.....(11)}$$

where k_B is the Boltzmann constant and N is the number of particles in the system. The number of degrees of freedom is $(3N - C)$, where C is the number of constraints such as constant temperature or constant momentum. Then the time average temperature will be:

$$T = \frac{1}{(3N - C)k_B} \left\langle \sum_{i=1}^N \left[m_i (\mathbf{v}_i - \mathbf{U}(\mathbf{r}_i))^2 \right] \right\rangle. \quad \text{.....(12)}$$

2.4.3 Determining local properties

Generally in MD simulation the averages are obtained for the entire space of the simulation box. However, in situations that involve non-isotropy and inhomogeneity, or when we are interested in the properties of the fluid on a certain point of space one needs to calculate the time average properties locally. For this purpose the volume of the simulation box is divided into a number of cells. To get good statistics each cell should be occupied by a few tens of particles. The properties that vary only in two dimensions are often calculated easily. This then involves dividing the simulation box in two dimensions into a number of sampling cells. This is shown in figure 4 for a flow over a cylinder of dodecane molecules.

All the local properties such as the stress tensor, velocity and density can be measured by this technique. Meshing in three dimensions has been attempted, but it requires much larger systems to acquire good statistics. There are subtleties in calculating the local stress from equation (10) as it involves pair-wise interactions and each atom could be residing on different sampling bins. In those situations the contribution to the stress is shared between the bins as a rough approximation. This has proved to work in practical terms.

2.5 Constant temperature and constant load simulations

Most of the instances where the rheology of the fluid is studied involve shear flow. In these simulations generated viscous heat must be removed somehow to ensure an isothermal simulation and to obtain a steady state. In homogeneous shear

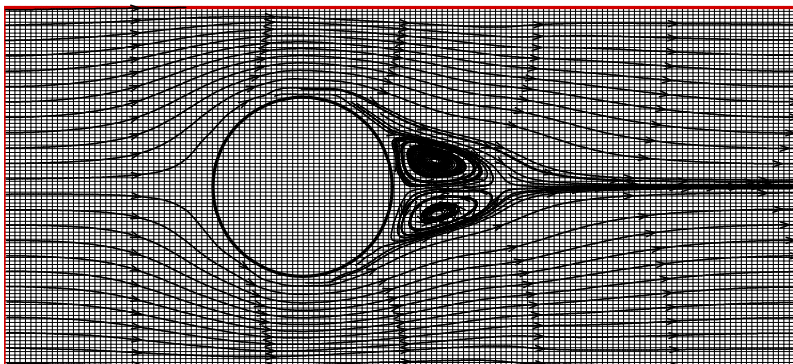


Figure 4: Flow over a cylinder in a rectangular box. The simulation area is meshed by a 150×100 grid. The calculated streamlines are also shown. The fluid is dodecane being simulated at 300 K and a density of 750 kg/m^3 . There are 40480 atoms in the simulation box. (A. Jabbarzadeh unpublished work)

simulations usually either a Gaussian thermostat [5] or momentum rescaling is used to remove the heat. The thermostat must be applied only to the thermal part of the velocities. That is the streaming velocity should be known. In bulk homogenous simulations using the SLLOD algorithm [5] a linear velocity profile is assumed so the thermostat is considered to be a profile-biased thermostat (PBT). Using a profile-biased thermostat at extremely high shear rates ($> \sim 10^{13} \text{ s}^{-1}$) is known to be responsible for transition to a ‘string phase’ in the simulation of atomic fluid [5]. It has been proved that a profile unbiased thermostat (PUT) [44], where the streaming velocity profile is calculated during the simulation, can remove this artefact. In boundary driven simulations of thin liquids film it is generally believed that the ideal way of removing the generated heat is to let it flow from the fluid to the walls. This is similar to what happens in nature and most probably in the experiments. Then if an atomic wall is used, it is required only to thermostat the wall atoms. This method, although it appears to be the ideal way to make an isothermal simulation will not guarantee a constant temperature at high shear rates.

Liem *et al.* [45] performed simulations to compare a homogenous shear simulation (using Lee-Edwards periodic boundaries) and also boundary driven simulations (using moving walls). They used momentum rescaling and thermostatted walls respectively to control the temperature. They showed both methods lead to identical results in cases where both converge to a steady state. However, for boundary driven methods, thermostating the walls worked only at lower shear rates for LJ fluids. The reason was that the fluid heated up to such an extent that the particles

penetrated the atomic wall. This problem appears to put a limit on utilising a conducted heat flow to the walls at high shear rates. Since the simulations at lower shear rates are prone to higher statistical uncertainties, and, on the other hand, simulations are not possible at high shear rates by conducting the heat to the walls, we will be limited to only a small span of shear rates that are possible to be simulated, if only a thermostatted wall method is used. In any case, it is desirable in some situations to examine very high shear rates. So in order to achieve high shear rate simulations a combination of thermostatted walls and thermostatted fluid may be used. Although the simulations are conducted at very high shear rates, the thickness of the fluid film is in the range of nanometres and the calculated Reynolds number ($Re = \rho \dot{\gamma} Z^2 / \eta$) is still very low. For example for a hexadecane film with thickness of $Z = 3.898$ nm at a very high shear rate of ($\dot{\gamma} = 10^{12.5} \text{ s}^{-1}$) the calculated Reynolds number is ~ 0.2 . This is much smaller than that expected for a turbulent flow. Even in the case of LJ fluid simulation at the highest shear rates the Reynolds number is less than 1000 which is the limit beyond which 'string phases' are expected to happen (10^3 - 10^5) [5]. For rigid model of molecular liquids it is found that using an atomic version of a thermostat instead of a molecular thermostat applied to the centre of mass of molecules can result in non-zero anti-symmetric stress [46]. Whether this is the case with the non-rigid molecules is unknown, however it seems unlikely, and the stress tensor obtained has proved, on checking, to be perfectly symmetric. Even for rigid molecules it is found that the results for atomic and molecular thermostats are identical for shear rates up to 1 in reduced units ($\sim 10^{11} \text{ s}^{-1}$ for alkane systems). It is only at extremely high shear rates that the results become different [46]. So as rule of thumb, the thermostating method is not going to make any difference in the results as long as one keeps the shear rate below 10^{12} s^{-1} .

Most of the experiments on confined liquid films are done under constant pressure or constant normal load (NPT simulation). This allows for the motion of the confining surfaces in the normal direction. In MD simulations constant volume methods (NVT) are much easier to implement, and in fact many simulations are done using this method. However it is believed that NVT and NPT simulations produce different results for the rheological properties with the latter having a smaller slope in the non-linear, shear thinning regime. This however, is to be expected, as the constant volume does not allow for dilation and at higher shear rates the normal stresses lead to increased pressure and hence different rheological properties from those found using constant pressure. One way of reducing the difference is to use an elastic wall with wall atoms attached to elastic springs, effectively allowing for the change in volume. Another method keeps the normal load constant by allowing the walls to move vertically by defining an equation of motion given by equation (13) for the wall in direction normal to the wall where ζ is a damping constant, and A is the area of the wall and P_{zz} and P_0 are the normal and external pressures.

$$\dot{z} = \zeta A (P_{zz} - P_0) \quad \text{.....(13)}$$

Other methods such as grand canonical molecular dynamics (GCMD) developed by Gao et al [47] can be used for maintaining the constant pressure, temperature and chemical potential. This method however requires a larger number of

molecules to be simulated because confined films are used in combination with a bulk region where the molecules in the confined region freely interact with those in the bulk region. The bulk region acts as reservoir at constant pressure. The problem with this method is that the confined region (with solid blocks) in one lateral direction is restricted to a very small strip that could be much smaller than those studied in the experiments. To reduce this system size effect one then has to choose a larger system that makes the method even more expensive. In other NEMD methods the size problem is usually taken care of through utilizing the periodic boundary conditions.

2.6 The scope of time scale and limitations

Although MD is used as a powerful tool in many applications, it has its own limitations and one should be aware about those before using it. The time scale involved in typical MD simulations is of the order of few tens of nanoseconds. This could be further diminished if the size and number of molecules under consideration are increased. A rheologist is usually interested in measuring mechanical properties such as stresses and viscosity under some sort of deformation such as planar Couette, Poiseuille and extensional flows. Two problems that arise here are related to thermal noise and relaxation times. At lower shear rates thermal noises are comparable to signals resulting from the perturbation and it is hard to resolve a reliable time averaged stress tensor due to large statistical uncertainty. For confined systems, if one is measuring the stresses through the forces on the wall less noise and hence lower statistical errors are found in the results. However there is still a limit for shear rate below which our readings will be meaningless. As the shear rate is decreased we need to run our simulations for longer times to get a reliable snapshot of the phase space and more reliable time averages. The problem is enhanced in the confined systems because the relaxation time of these systems is increased significantly because of confinement effects. Usually the maximum reasonable time one can run a simulation for a typical number of 10000 atoms is 100 nanoseconds (ns). The Rouse model can be used as a measure of the critical shear rate ($\dot{\gamma}_c$) for the start of non-linear behaviour (that is when the shear thinning begins). We know $\dot{\gamma}_c$ is inversely proportional with the relaxation time (λ), (ie. $\dot{\gamma}_c \propto 1/\lambda$). A simulation time limit of 100 ns translates to a shear rate of $\sim 10^7 \text{ s}^{-1}$. That means if the relaxation times are larger than this then we will not see a Newtonian plateau for the system through our NEMD runs. So the NEMD simulations will provide shear viscosities and not zero shear rate viscosity (η_0 , Newtonian viscosity) if the relaxation time of the molecules are beyond the reach of our simulation time. In some cases, however, extrapolation of the results can give us an indication of the viscosity at the lower shear rates. Using the Green-Kubo [6] technique through equilibrium molecular dynamics is another approach to calculate the zero shear viscosity. However that also involves an upper limit of integration time that the results are sensitive to. This upper limit should be within the relaxation time of the system and hence simulation time constraints as in NEMD simulations are also applied here. Despite these limitations, there are promising approaches to improve these shortcomings. Among those new trends we can mention the transient time correlation function (TTCF) method [48] that makes it possible to use MD simulations for viscosity calculations at lower shear rates, and the momentum impulse relaxation

method [49] that provides a computationally faster and more efficient method for viscosity calculation.

3. FLOW IN NANO-CHANNELS AND THIN LUBRICANT FILM RHEOLOGY

3.1 Experimental studies of thin film rheology

Intriguing experiments on ultra thin lubricant films have inspired simulations in nano-channels. Bailey and Courtney-Pratt [50] pioneered these experiments, and decades later their experimental method was improved with the invention of the surface force apparatus (SFA) by Israelachvili and Tabor [51] who measured the shear properties of thin films. Chan and Horn [52] measured the film thickness of three non-polar organic liquids, including n-hexadecane, as they squeezed them between atomically smooth mica surfaces. They found that the Reynolds theory of lubrication worked well only for film thicknesses down to 50 nm. The experimental work of Israelachvili and his co-researchers pioneered this area [53-55]. Early measurements by Israelachvili [53] for pure liquids, water and tetradecane, suggested that viscosity remains constant within about 10% of its bulk value down to a film thickness of 5 nm. However other measurements [56] for cyclohexane with adsorbed polymer layers onto the surfaces showed that the viscosity could become 20 times larger than that of the bulk viscosity at wall separations of the size of the radius of gyration of the adsorbed polymer. Measurements for crude oil [54] and experiments with PDMS (polydimethylsiloxane) and OMCTS (octamethylcyclotetrasiloxane) also found similar increases in the viscosity. Experiments on various types of liquids suggested that the static and dynamic properties of the molecularly thin liquid films are very different from those of the bulk liquid [57]. Oscillatory force measurements between two mica surfaces [58, 59] indicated strong layering between the surfaces. Perhaps one of the most extensive studies on these confined films has been conducted by Yoshizawa and Israelachvili [60-63]. Doing experiments on linear chain molecules of alkanes and globular shape molecules they have observed a rich range of phenomena that include increased relaxation time and viscosity for these confined films together with stick-slip behaviour that changed patterns with the type of molecules, load and temperature. These films show remarkable memory effects which are an indication of resilient molecular orientation due to very large relaxation times and trapped metastable states. These works suggest that there exists a critical temperature at which a stick-slip motion between two mica surfaces separated by a 1.2 nm film of hexadecane changes to a smooth motion. This critical temperature was suggested to be dependant on the film thickness and twist angle between the crystallographic directions of the two mica substrates. The stick-slip friction force was shown to decrease with the temperature. The temperature in these experiments with hexadecane was very close to its melting point ($\sim 18^\circ\text{C}$) so it was hard to separate the effect of confinement induced order and temperature induced freezing. The stick-slip frequency was also shown to be increasing with the shear rate and beyond a critical shear rate the stick-slip disappeared. It is suggested through MD simulation [64] and theoretical methods [65] that the stick-slip is the result of periodic solidification and subsequent melting of the confined film. There are some limited experiments that also show the alignment of the confining

surface with each other can affect the results. Two fully aligned (zero twist angle) surfaces have been shown to result in higher friction both for bare mica [66] and a confined film of tetradecane [63] and also liquid crystals [67] have shown that higher shear stresses are observed for fully aligned surfaces. Even a small twist angle $\sim 10^\circ$ can reduce the shear stress and make the stick-slip disappear [63]. While transition to a kinetic friction is observed with disappearance of stick-slip for a film with freely moving molecules such as hexadecane, an extremely low friction (superkinetic state) can be seen with grafted type molecules [62].

Granick and his co-workers [68] also have done extensive experiments with various liquids ranging from simple molecular liquids to polymer melts. They measured the oscillatory shear response of the liquid films with a thickness of 1-6 molecular diameters at shear rates ranging from 10 - 10^5 s^{-1} . They observed a solid-like response with yield stress and a liquid-like response where no critical shear stress was observed for starting the motion. The measurements gave an enhanced effective viscosity compared to that of the bulk liquid. It was also shown that the viscosity was extremely dependent on the film thickness and the normal pressure. In a later study [69] it was found that this critical stress was a source of static friction, which could build up over time and was enhanced by normal pressure. For polymer melts [70] the transition times between liquid-like and solid-like behaviour could be of the order of seconds to minutes although the general behaviour would be the same. The Hu *et al.* [71] experimental work on the shear response of chain molecules of dodecane and also OMCTS for film thicknesses of 3-10 molecular diameters is a classic work in the field. In this work they used oscillatory shear to probe the rheological properties of these thin films. The measurements of apparent viscosity over shear rates ranging from 1 - 10^5 s^{-1} for dodecane at a film thickness of 2.7 nm (6 molecular diameters) and OMCTS at the same thickness indicated shear thinning. The apparent viscosity obeyed a power law of the form $\eta \propto \dot{\gamma}^{-2/3}$. The power increased in absolute value with decreasing film thickness with an increased net normal pressure. At all shear rates the viscosity was larger than the viscosity of bulk fluid, but shear thinning resulted in a decrease of viscosity by more than two orders of magnitude. Also, a general increase in the viscosity with decreasing film thickness was observed. This was in general agreement with previous findings for hexadecane [68-70, 72]. The critical shear rate for the onset of shear thinning also decreased as the film thickness was reduced. One of the important findings was that the Newtonian zero shear rate viscosity was 5-6 orders of magnitude larger than that of bulk dodecane. Study of nano-rheology of larger molecules of polymer melts of PPMS (poly(phenylmethylsiloxane)) confined between strongly adsorbing surfaces of mica by Granick and Hu [73] showed similar observations. For different chain lengths it was found that both the shear moduli and the applied normal force to squeeze the film to the required thickness scaled up with the radius of gyration of the chains. It was also suggested that the measured value for the storage shear modulus indicated an enhanced entanglement of the chains in those strong adsorption limits. Large amplitude non-linear shear rheology of the same polymer melts was also studied at strongly adsorbing surfaces [74] and weakly adsorbing surfaces [75].

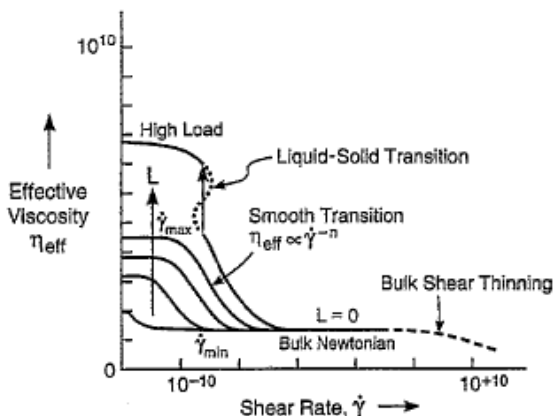


Figure 5: Proposed generalized map of effective viscosity [76] (Reprinted figure 4 from *Wear*, V 200 by Luengo G, Israelachvili J and Granick S, “Generalized effects in confined fluids: New friction map for boundary lubrication”, 328-335, Copyright (1996), with permission from Elsevier).

Based on these experimental observations an effective viscosity map was proposed by Luengo et al [76]. This is shown in figure 5. In this figure we can see that at zero loads corresponding to bulk liquid elastohydrodynamic sliding regime the shear thinning only happens at sufficiently large shear rates. Increasing the load and subsequent transition to boundary lubrication regime, results in much higher effective viscosity with Newtonian behaviour at low shear rates. At higher shear rates non-Newtonian behavior with characteristic shear thinning sets in with a power law behaviour in the form of $\eta \sim \dot{\gamma}^n$ with n having values between -0.5 to -1 that increases in absolute value as the load is increased, (reduced film thickness). This trend (dependence of n on the film thickness) is confirmed by simulations and experiments [77, 78]. The onset of this shear thinning regime for boundary film is suggested to be discontinuous accompanied by various stick-slip patterns. This regime is followed by a second plateau of Newtonian regime. Increasing shear rate further leads to a secondary shear thinning regime.

Recent experiments [79] show these films exhibit distinct stick-slip behaviour with transition to lower friction sliding for simple lubricants and melts [78]. The state of this transition seems to be dependant on the molecular type of the lubricant. While linear alkane and simple lubricants show abrupt transition, branched alkanes show a continuous transition. As the sliding velocity is increased the film jumps from one steady state with high viscosity to another steady state with a lower viscosity [80].

These experiments showed at shear rates accessible in the lab (typically $< 10^5 \text{ s}^{-1}$) it took a few minutes for the film to get to a steady state smooth sliding regime. One would imagine as the shear rates are increased this should take less time. With the advance of experimental techniques such as new generation of SFA that take advantage of in situ x-ray diffraction and also using AFM it is possible to probe the structure of the confined films. Shear induced crystallization, and aligned phases on the boundary [81] and within the domain [82] that form with a $\sim 42^\circ$ angle with respect to the shear direction are reported for confined films of n-eicosane, a linear alkane. Despite ongoing research in this area for almost a decade there are still many unresolved issues. Disagreement between the experimental results is not uncommon with some recent experiments challenging some of the older findings [83, 84].

The nature of the transition to the high viscosity regime is still a matter of debate. While some of the results suggest a continuous transition as the film thickness is decreased to 6-10 molecular diameters [71] recent experiments by Klein and Kumacheva [85] on OMCTS suggest an abrupt transition. We are still only beginning to understand the correlation of film molecular orientation and rheology. There are many issues that still beg for the attention of the experimental research community in this field. It is not still clear whether the observed phenomena are the result of using a particular type of surfaces which in most cases is formed from cleaved sheets of atomically smooth mica. Although it has been suggested the behaviour is universal regardless of the type of molecules and surfaces [86] more recent results shed doubts on this universality. The experimental procedure for probing the rheological properties can be divided in two categories. Those that use oscillatory shear and those employing steady shear (no directional change). In normal circumstances for measurement of bulk rheological properties this should not make much difference. However these films exhibit properties that sometime are dependant on the time and distances that they go under continuous shearing. We are beginning to understand that every little detail counts on these experiments. Issues of surface contamination [84], method of preparation, the type of the surfaces and their relative orientation and crystallographic direction and shearing directions seem to be of crucial importance. So any comparison of the experimental results should consider these subtle differences. Some of these fine points are simply beyond the capabilities of current experimental techniques. It is exactly at these circumstances that computational methods such as MD present themselves as a tool to shed light of these complex problems.

3.2 Molecular dynamics and thin films

A molecular level study of flow near a solid surface is essential for understanding the mechanisms of spreading, wetting, lubrication, polymer coating and processing, friction and thin film casting. These important applications in engineering and science make the study of the thin liquid films both rewarding and interesting.

Computational investigations of flow near solid walls usually are carried out to complement the experimental findings and to explain some of the observed phenomena that cannot be explained in experiments. The advantage of the simulations over experiments is that one has detailed control over conditions under which a problem is

investigated. In the laboratory however there are many issues such as contamination, surface and film preparation methods that may affect the results and controlling them from one experiment to other can be troublesome. In the simulation also some information regarding the dynamics and structure of the film can be extracted that is usually not possible in the laboratory.

The simulation of thin confined films, which is the main focus of our attention in this article, can address a wide range of issues including:

- 1 - The nature of transition to high viscosity regimes;
- 2 - The source of the transition;
- 3 - Transport and dynamic properties of the film before and after transition;
- 4 - Effect of the surface topology, structure and properties on the film rheology and response;
- 5 - Origin of stick-slip;
- 6 - Parameters that affect the boundary conditions;
- 7 - Effect of the fluid molecular structure on the properties and response of the film;
- 8 - Devising practical methods to manipulate the rheological behaviour of the film.

3.2.1 Historical perspective, from simple to complex systems

Computer simulation has been employed as a powerful tool in investigating the flow behaviour in molecularly thin film liquids. These simulations have been able to capture unprecedented detail about the film behaviour and have been able to reproduce some of the experimental observations and more importantly to explain the nature and origin of such observations. Although all computer simulations have many distinct features, most of them use molecular dynamics techniques in their simulations. These simulations can be categorised in different groups:

1. Simulations which investigate the equilibrium properties of the confined films (no flow is considered);
2. Simulations which study the thin liquid film properties in some kind of flow geometry (The most popularly studied kind of flow has been Couette flow between two planar surfaces. However, some researchers have investigated Poiseuille and squeezing flows as well);
3. Simulations which use simple atomic fluids with soft, Lennard-Jones spheres;
4. Simulations which analyse more complex macromolecules, like polymer melts. These include branched molecules, ring shaped molecules and so on.

The simulation of thin liquid films can also differ in many other technical details and also in the chosen molecular model. For instance the model for the solid surface can be chosen to be a smooth and structureless wall, or a wall constructed of individual atoms. Thermostatting methods for simulations conducted in isothermal conditions can also vary from one simulation to another. Using these simulations we have realised that inhomogeneity with marked variation of density over molecular distances is a trademark of molecularly thin films that distinguish them from the bulk. This strong variation leads to ordering of the fluid molecules and hence significantly different properties from that of the bulk material. We are beginning to understand the nature of such transitions. The simulations have generally revealed the solid-like behaviour of fluid layers near the walls, a phenomenon that could even lead to the crystallisation of the entire film when the wall separation was less than 5-6 molecular diameters, leading to a finite yield stress [87]. According to these studies, in films narrower than three to four molecular diameters flow is dramatically different from that of bulk fluids [89]. In sufficiently thin films and at high shear rates the measured viscosity decreases with shear rate, obeying a power law with an exponent of -0.5, which implies a shear thinning effect. This happens independently of the molecular composition of the film [87]. We will review some of these computational findings in the coming sections.

Molecular dynamics simulations of fluids in narrow channels have been carried out since the 1980's. Bitsanis and co-workers did simulations [89] mainly for fluids in pores. Magda *et al.* [90] performed MD simulation for a 6-12 Lennard-Jones liquid in channels about 2-12 molecular diameters wide. In this work smooth walls were used as a model so that the potential between each particle and the wall depended on the normal distance of that particle from the wall. Bitsanis *et al.* [42] introduced a local average density model (LADM) of viscosity and diffusivity in which the local transport coefficients were those of homogenous fluid at mean density obtained by averaging the local density over a molecular volume. According to Bitsanis this model predicted qualitatively correct values for velocity profiles, effective viscosity and shear stress. The LADM model was used to set up the mechanical equations for Couette flow, Poiseuille flow and squeezing flow between parallel plates. According to this analysis different equations could be derived for the effective viscosity depending on the flow type [91]. The results for velocity profiles, stress distribution and effective viscosity showed strong correlation between these properties and the density variation across the channel. Also the dependence of viscosity on the nature of flow was highlighted [91]. Although the LADM model seemed to be valid for some narrow channel flows, further studies [89] showed that in films narrower than three to four molecular diameters flow was dramatically different from that of bulk fluids and could not be explained by a local average density model (LADM). This different behaviour, especially the enhanced viscosity, was explained by the inability of fluid layers to undergo the gliding motion of planar flow. In other words the increase in the effective viscosity was explained to be the result of fluid layering not as a consequence of the average density rise. Some interesting simulations have also been carried out for examining the non-slip boundary condition in flows next to solid walls [87, 88]. These simulations were performed for Couette flows between two planar solid walls. The liquid was a simple LJ fluid consisting of spherical molecules. Stronger interaction between wall and fluid was shown to induce the fluid layers to become narrower and closer to the walls. It was also demonstrated that increasing the density of the atomic wall

could affect the fluid layers only by sharpening their profiles but did not make them closer to the walls. In planar Couette flow simulations it was found that normal stress was not constant on the atomic scale contrary to what is expected from the Navier-Stokes equations. This oscillation in normal stress and also the velocity gradient across the slit was of the order of a molecular diameter and averaging normal stress and velocity on this scale would remove the oscillations [88]. Beyond the first or second layer these average values would satisfy the Navier-Stokes equations with a constant viscosity. In the same work the degree of wall slip was shown to decrease with increasing wall-fluid interaction strength. More recent results reported [77] the degree of slip increasing with shear rate. Thin fluid films of flexible chain molecules sheared between two solid walls were also investigated [87]. The fluid consisted of spherical molecules or flexible linear chains of up to 20 monomers connected by FENE type springs and the walls were atomic, structured from the (111) plane of a FCC lattice. The atoms were coupled to lattice sites by means of stiff springs. The simulations were done with a constant pressure applied to the walls. To find the dynamic response the film was sheared by moving the upper wall at a steady velocity and then the mean frictional force per unit area was found. Their results [87] showed that at high shear rates there was a substantial shear thinning with the viscosity obeying a power law. Also they showed that, below a characteristic shear rate $\dot{\gamma}_c$, the viscosity saturated to a limiting value and that the film exhibited bulk-like dynamics down to a thickness of 6 molecular diameters. At smaller separations it was found that there were dramatic increases in the relaxation time and the viscosity. This kind of increase was attributed to a confinement-induced glassy transition. Another important finding was that in the non-Newtonian regime for these glassy films where $\dot{\gamma} > \dot{\gamma}_c$, the viscosity obeyed a power law in the form of $\eta \propto \dot{\gamma}^{-2/3}$ [87], suggesting it could be a universal property of lubricants near a glassy transition under constant normal load. At constant wall separations however this relationship was less universal with $(-2/3)$ replaced by $(-1/2)$. The reason given was that the film could not expand to facilitate shear at constant film thicknesses. In the case of flexible chain molecules it was suggested that the chain length had no effect on the viscosity of the film, although it increased rapidly with chain length for bulk fluid. However more recent results concluded differently about the effect of the chain length [92]. This work suggested that the long relaxation time and increase in viscosity is the result of wall-induced glassy transition. Lupkowski and Van Swol [93, 94] investigated properties of thin film liquids in two different geometries. Their first work simulated the confined fluid interacting with fluctuating walls [93] and the second work was on the simulation of planar shear flow [94]. In the earlier work [93] the particles were placed in a rectangular box with two rigid walls at two opposite faces. An external pressure was put on the walls so that walls could fluctuate and mimic a constant pressure system. In these works it was shown that the wall-particle mass ratio had an effect on the equilibration time and fluctuations in pressure but had no effect on final statistical averages. The simulations were done for both hard and soft spheres. The results suggested a lower value for wall-particle mass ratio for short time scale fluctuations and hence better sampling of phase space. In their later work [94] they examined the shear flow of thin liquid film between two walls with fixed normal load on the top of the walls. The material between the plates was allowed to exchange particles with an external reservoir during the shearing process. The model replicated the experimental technique developed by Israelachvili [95] and

consisted of two atomic walls one of which was attached to a spring and the other was moving with a constant velocity. The shear force then could be found from $F_s = k\Delta X$ where ΔX was the deviation from the equilibrium position of the surface which was attached to the spring. The results for the shear flow indicated stick-slip behaviour for low shear rates accompanied by a gradual increase in stress and then a sudden and sharp decrease in stress and decrease in the number of particles. A sudden increase in wall separation was also observed in this situation. For higher shear rates it was shown that the system moved to a pure sliding regime. Profound effects of the walls on the fluid structural and dynamical properties such as the self-diffusion coefficient have been observed [96, 97]. Heinbuch and Fischer [98] studied the behaviour of the fluid in Poiseuille flow for a cylindrical pore. A cylindrical wall was formed by regularly arranged fixed atoms of 16 rings each of 25 equally spaced atoms. The cylindrical atomic pore had a radius of about 5 molecular diameters. The driving force which induced the Poiseuille flow along the cylinder axis was assumed to be of the gravitational form with an acceleration $g = 0.1$ or 1.0 (in reduced units, $\epsilon/m\sigma$). Analysis of the results revealed that the molecules in the first adsorbed layer were in register with the triangular lattice of the wall atoms and that the second layer was strongly structured. Comparing velocity and density profiles for different runs also provided some information regarding the effect of temperature, driving force, wall attraction strength and heat-dissipation mechanism on the structure of the flow and velocity field. Apparently temperature had little effect on the velocity in the case of a weakly attractive wall. However for a strongly attractive wall increasing the temperature removed the second adsorbed layer and made it flow. Increasing the driving force from $g = 0.1$ to $g = 1.0$ made the drift velocity ten times larger and the second layer did not stick to the wall. This showed that higher driving forces could sweep away the sticking layers. One of the works that needs to be mentioned here, although not directly related to thin liquid films is the simulations of Liem *et al.* [45]. Their work contains some useful information on the technical aspects of this kind of simulation. They did some simulations with LJ particles to examine the shear flow with sliding solid boundaries and compared it with the homogenous NEMD shear flow, which used the Lees and Edwards [17] sliding periodic boundary method. They computed the local stress tensor components from the wall dynamics and also from the virial theorem and compared it with the results at the same local shear rate for the homogenous shear model. The distance between the walls was large, about 50 molecular diameters. A slicing method was used to calculate the streaming velocity and other local properties. However it seems that in the calculation of the stress tensor components from the virial theorem they ignored the contribution of the wall particles to the configuration part of the stress tensor. They encountered also problems at very high shear rates, when fluid particles penetrated into the solid walls.

A study by Bitsanis and Hadzioannou [99] investigated the behaviour of confined polymer melts in the vicinity of solid walls and sought their equilibrium dynamic and static properties. Flexible chain molecules consisting of up to 30 segments were studied. A truncated shifted 6-12 Lennard-Jones potential together with a 10-4 LJ wall potential were used for fluid-fluid and wall-fluid interactions respectively. By choosing proper values for the energy parameter of the wall potential three types of smooth walls were examined including purely repulsive and short range, weakly attractive and strongly attractive walls. A FENE (Finitely Extendible Non-linear Elastic) spring was used to

connect the segments of the same molecule. The isothermal condition was maintained by scaling the segment velocities at each time step. The results for density profiles indicated that the peak density near the walls was quite low compared to the simple spherical liquids and the density oscillations were dampened much more strongly in the case of polymer melts. The study of the chain orientation in the liquid slabs showed that bonds preferred to be more or less normal to the walls over 2σ - 3σ distances from the wall [99]. This trend was especially strong for short chains. For larger distances, however molecules were randomly oriented. By defining an end enhancement factor a preferential adsorption was observed for the end beads of the chain molecules. This means, very close to the walls, that the density of chain ends was very much higher than the density of other beads. By averaging this enhancement factor over the interfacial region (2.5σ) it was found that the deviation of the end density from the other beads' density occurs only in this narrow interfacial region. Nevertheless, in the presence of a strong attractive wall the tendency of the chain ends to accumulate close to the walls was reduced as a result of having the middle beads inside the well (attractive tail) of the wall potential. It was shown that the shape of the chain portion in the interfacial region could be severely distorted. In this region the chains tended to lie flat on the surface but the shape of the rest of the chain was unaffected outside this region. This phenomenon resulted in apparent shrinking of the chains normal to the walls and apparent swelling parallel to the walls. However, the overall length of the chains in the interfacial region was close to the bulk value throughout the film. The dynamic properties of the polymer melt inside the interfacial region showed the bead mobility was higher than the bulk value parallel to the wall and lower than the bulk value normal to the wall. This was, however, attributed to the layering of the beads for the formation of the interface. Also the mean square displacement of the chain centre of mass over a certain time interval was shown to be anisotropic and different from the bulk value for the chains which had some portion of themselves in the interfacial region. Bitsanis and Hadziioannou [99] argued that the effect of the walls was localised and very short range. They also argued against the existence of any forces between the solid surfaces intermediated by polymer melts and against the existence of profoundly different rheological behaviour of polymer melts within a distance of one radius of gyration from each wall, such as was inferred from some experimental results.

They also studied [100] the equilibrium properties of confined films with shorter chains with 5 segments in each molecule. Their simulation for different solid wall interaction strengths suggested that there was a large increase in the relaxation time of the chains in the adsorbed layers close to the solid surfaces. They suggested strong crowding of the segments in the adsorbed layer were responsible for this effect. They also suggested that this slow dynamics of the adsorbed layers could be the reason for the increase in the viscosity of the thin films. However this would happen for very thin films where the adsorbed chains comprise a significant portion of the confined film. It was suggested, for thicker films the free chains are the substantial portions of the film, so not much deviation from the bulk viscosity is observed.

In the work of Manias *et al.* [101], which seems to be a follow-up to the above mentioned work, the behaviour of polymer melts under shear was investigated. The simulations were performed for Couette flow geometry by confining the polymer melts between two parallel walls, which were moving with constant velocity in opposite

directions. For more attractive walls the density inhomogeneity was found to be stronger. The shape of the flow velocity profile across the channel showed a strong correlation with the density profile. The velocity profile was linear only in the middle part of the film where the density was almost constant. For the more attractive wall the first layer stuck on the wall. The simulation verified that for less attractive walls there was some slip between the walls and the first layer. This slip increased with increasing shear rates or with lowering the wall-to-wall distance. For more attractive walls much higher shear rates could be applied since the slip between the walls and fluid was negligible, though even for attractive walls slip could be observed for high shear rates. No dramatic change in the density profile was observed for less attractive walls as the shear rate was increased. However, for more attractive walls there was a systematic change in the density profile with the change in shear rate. In this case an increase in the density of the first and particularly the second layer was observed while the low-density area between these two layers decreased in density. These changes were attributed to the flat orientation of the chains, which were in contact with the walls. This kind of orientation increased the slip between two layers. This was confirmed by an observed increase in the fraction of beads in a molecule in contact with the walls. Manias *et al.* [101] suggested that the slip both between the wall and the fluid and between the interfacial layer and middle part occurred in the low-density areas where different parts of the system met. All the above-mentioned simulations for bead-spring type chain molecules lacked the intramolecular architecture including bond angles and dihedral potentials, which are the natural part of real polymer molecules. This fact made it difficult to decide if these “necklace” chains would behave like real polymers [100].

One of the important features of thin films is their ability to withstand the huge loads even when the thickness of the films goes down to only a few nanometres. In simulations of confined films of various alkanes such as hexadecane and squalane it is shown that the existence of normal stress differences is the main factor that make it possible to withstand such high loads. Figure 6 shows N_1 (first normal stress difference) and its ratio with the second normal stress difference $|N_1/N_2|$ for various linear and branched alkanes. At shear rates less than $\sim 10^{10} \text{ s}^{-1}$ that is the threshold of the nonlinear behaviour, N_1 is positive and $|N_1/N_2| \sim 1$, at higher shear rates in the non-linear regime, N_1 grows significantly and faster than N_2 . Note in these [102] simulations the thickness of the film was ~ 18 molecular diameters and thicker than the limit (6-10 molecular diameters) where “solid-like” transition occurs for the confined films. The generated first normal stress difference basically applies a normal force on the surfaces and keeps them separated while they are being sheared. The simulations have shown N_1 grows with effective length of the molecules [103].

3.2.2 Recent works

More realistic models for chain molecules have started to emerge in the literature in the simulation of simple hydrocarbons and alkanes. The parameters used in these simulations are well refined and is known to produce physical properties very close to that of experimental measurements [77, 104-109]. These simulations are now trying to tackle more complex real systems. The models chosen for both the wall and the confined fluid

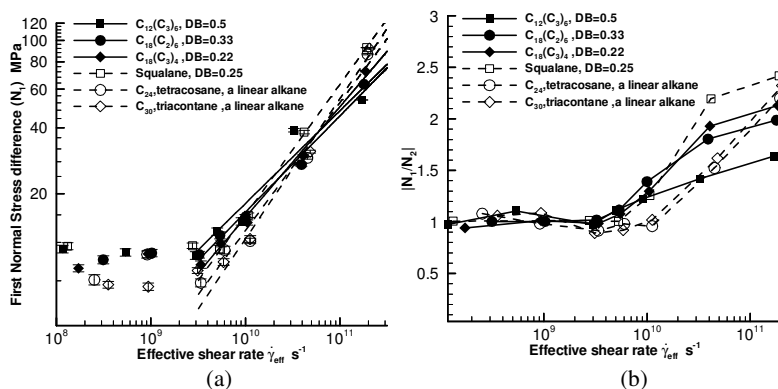


Figure 6: (a) First normal stress difference and (b) absolute ratio of first and second normal stress differences shown for various branched and linear isomers of $C_{30}H_{62}$ and also linear molecules of tetracosane ($C_{24}H_{50}$) alkane. The film is 7.2 nm thick (~ 18 molecular diameter) and above the limit where the film acts solid-like [102] (Reprinted from Tribology International, V. 36 by Jabbarzadeh A, Atkinson J D, and Tanner R I, “The effect of branching on slip and rheological properties of lubricants in molecular dynamics simulation of Couette shear flow”, 35–46 Copyright (2002), with permission from Elsevier).

although still not perfect, nevertheless mimics the mica-alkane system very closely. The potentials used for the alkane system can now predict a value of the viscosity of the alkane system very close to its experimental value [106].

3.2.3 The nature of rheological transition in thin films

All the experimental and simulation work points to dramatic changes of confined film properties with respect to those of the bulk. However what triggers these marked differences remains elusive. In the past few years some interesting refinements of the simulation methods that make the simulated models much closer to the experimental systems has helped to shed some light on the problem. Cui et al [107-109] in simulation of confined dodecane systems have shown that if wall-fluid interaction strength is set to values close to that of mica, provided the simulations run long enough, the equilibrated confined films 6 molecular layers thick or thinner form into distinctive layers packed in a form shown in figure 7. The molecules are accommodated in 6 distinctive layers and in each layer the molecules are highly ordered into mosaic-like domains in which they lie parallel to each other. The direction of the molecular axis in each domain is either parallel

or perpendicular with those in the other domains. Each domain is extended across the film and effectively forms a crystalline bridge [110].

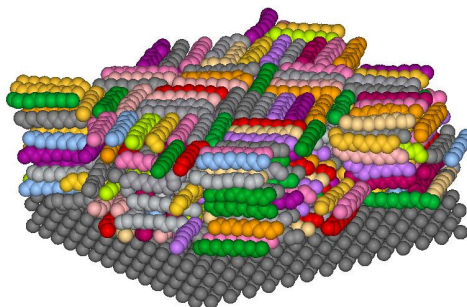


Figure 7: Snapshot taken for the 6-layer film of dodecane confined between two mica walls. (Top wall is not shown for clarity).

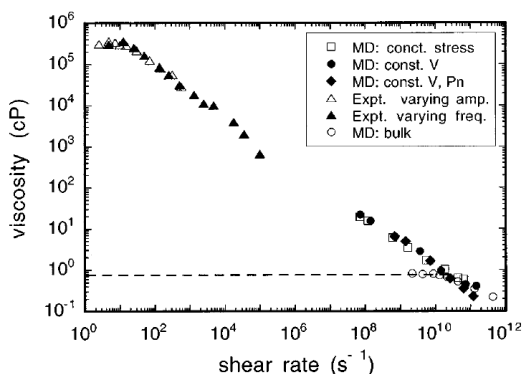


Figure 8: The calculated and experimental viscosity of the six-layer n-dodecane film vs. effective shear rate on log-log scales for constant-stress (squares) and constant-velocity (solid circles) simulations at constant film thickness; constant-velocity simulations at atmospheric normal pressure (diamonds), experiments (triangles), and calculated bulk viscosity (open circles). The dashed line indicates the constant Newtonian viscosity plateau of bulk dodecane. Experimental data were taken from the published work of Granick *et al* [71]. Open and solid triangles represent amplitude varied at constant frequency and frequency varied at constant amplitude respectively. Reproduced from Cui *et al.* *J. Chem. Phys.* (2003) [109].

The transition to this highly ordered configuration is suggested to be the result of increased effective density by Cui et al. Measuring the shear viscosity for a 6 layer film of dodecane they have shown their extrapolated results are similar to those measured by Hu and Granick [71] at lower shear rates [109]. This is shown in figure 8.

Using the work of Cui et al as a base for our own study we have been able to conduct one of the most comprehensive studies to date on the confined film rheology of dodecane films. The result obtained through these simulations address some of the issues that have been debated over the last two decades. Presenting some of these results here we will put forward some of our conclusions as an answer to some of these questions.

The nature of the transition to high effective viscosity regime lies in the structure of the film between the solid surfaces. It is this structure that dictates the rheological response. For the dodecane film the process that led to the formation of this mosaic-like in-plane order which stacks across the film is very interesting. We have conducted isothermal, constant normal load simulations at 300K and 1 atm, for various film thicknesses starting from films 4.45 nm down to 1.98 nm.

The snapshots of the equilibrated films 2.85, 3.95 and 4.45 nm are given in figure 9. For films 2.85 nm and thinner the equilibrated film has a mosaic-like structure. The shear response for these films corresponds to a very high effective viscosity as shown in figure 10 and is in agreement with those reported by Hu et al. [71]. For films 4.45 nm and thicker there is no organization at the middle of the film, although the layers next to the walls retain the same mosaic-like structures. For this film the viscosity is very close to that of the bulk dodecane (see figure 10). For a film in the intermediary region with 3.95 nm thickness (figure 9b) there are bridges formed between the walls. These bridges are surprisingly resilient to the applied shear rates. From the animations produced we can see at a shear rate of 10^8 s^{-1} the bridge distorts, then detaches itself from one surface at a point a few layers away from the wall and reattaches itself to some suitably ordered surface layers in a reduced strain configuration. We find that the bridges are destroyed at shear rates $\geq 10^9 \text{ s}^{-1}$. The shear-induced destruction of the bridges is reversible so that when the shear rate is reduced back below 10^9 s^{-1} we observe the formation of new bridges. The viscosity behaviour corresponds very well with these structural formations. As we can see in figure 10 for 3.95 nm film a higher viscosity is registered at lower shear rates where these bridges still exist. The viscosity though is still smaller than that of a 2.85 nm thick film whose mosaic-like structure in the form of multiple interwoven bridges are formed. The sudden drop in viscosity for 3.95 nm film corresponds to the point where these partly formed crystalline bridges are destroyed.

The nature of the transition itself is a matter of debate where a continuous transition is suggested by Granick and his co-workers [71]. A sudden discontinuous transition is favoured by Klein and Kumacheva [85]. Our results points to a discontinuous transition due to the structural pattern formed in the film. Despite suggestions of freezing transition and “solid like” transitions our results show an evolving film which is far away from freezing or being solid. The calculated diffusion coefficients show a significant slow down in the dynamics. At that point there is a break-up between viscosity and inverse diffusion linear relationship, characteristic of a

liquid [110]. However, diffusion is still bigger than what would be expected from a solid material. Our further work on temperature [110] and shear induced transitions to a disordered phase also favours a discontinuous transition.

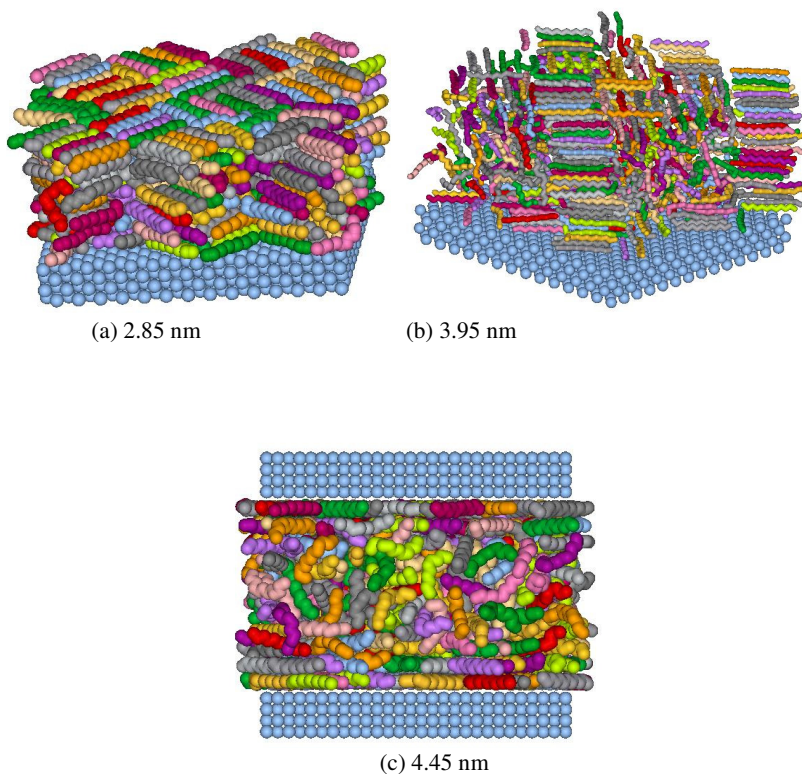


Figure 9: Snapshots of simulated confined dodecane films between model mica surfaces under constants temperature and load conditions of 310 K and 1 atm for various film thicknesses. The top wall in some cases is not shown to ease the visualization of the formed structures.

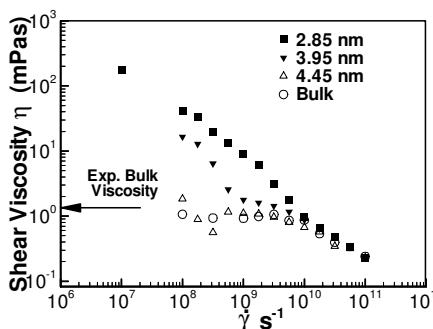


Figure 10: Effective shear viscosity against the shear rates for various film thicknesses for dodecane at 300 K and 1 atm normal load pressure. The simulated bulk viscosity is very close to the experimental measurement. The 2.85 nm film is a 7 layer film with mosaic-like structure. The 3.95 nm film correspond to a film with partially formed crystalline bridges. For the 4.45 nm film except for the two layers next to the walls, there is no ordering. Note the sudden drop in viscosity for the 3.95 nm film. The drop corresponds to the stage where the bridges are destroyed due to applied shear.

An example of a shear induced melting and transition to disordered phase are displayed in figure 11. In this figure g_2 and g_4 [111] are second and fourth rank correlation functions defined as:

$$\begin{aligned} g_2(r) &= \langle \cos 2[\theta(0) - \theta(r)] \rangle \\ g_4(r) &= \langle \cos 4[\theta(0) - \theta(r)] \rangle \end{aligned} \quad \text{.....(13)}$$

These two parameters are widely used in structural analysis of liquid crystals. Where $g_2 \approx 0$ and $g_4 \approx 1$ is an indication of tetratic order (mosaic-like structure) and $g_2 \approx 1$ and $g_4 \approx 1$ is an indication of nematic order (parallel alignment). $g_2 \approx 0$ and $g_4 \approx 0$ indicates there is no particular order and molecules are aligned randomly. The film presented in figure 11 starts from a mosaic-like structure that is signified by $g_2 \approx 0$ and $g_4 \approx 1$. This stage is associated with high shear stress and stick-slip spikes with large amplitudes. The shearing results in destruction of the mosaic-like order and crystalline bridges across the film. The film is expanded with increased thickness and transition to smoother lower shear stress values that is reminiscent of the “kinetic friction” regime.

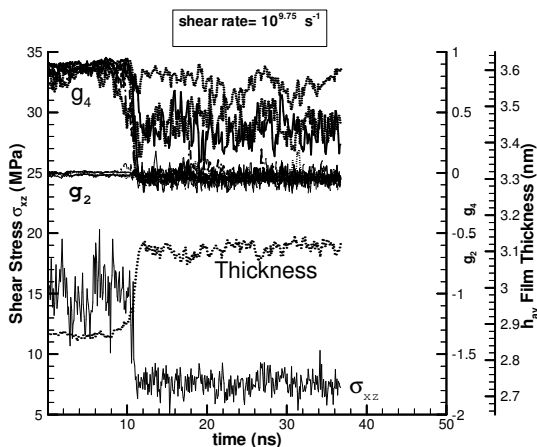


Figure 11: Shear induced transition of a mosaic-like ordered structure film 2.85 nm thick to a disordered film. This increase in disorder results in the increase of the film thickness and decrease of shear stress. The orientation order parameters g_2 and g_4 show the signature of this transition ($g_2 \approx 0$ and $g_4 \approx 1$ is an indication of tetratic order (mosaic-like structure) and $g_2 \approx 0$ and $g_4 \approx 0$ is an indication of no particular order).

3.2.4 Multiple rheological states

Using very long runs we have recently shown that dodecane films confined between model mica surfaces are capable of demonstrating multiple rheological states [106]. Figure 12 shows this transition to low shear viscosity regime. The film is 2.8 nm (measured from the position of the wall atoms) thick initially and equilibrated with a strongly layered structure as shown in figure 7. Starting from this equilibrated film, applying shear initially destroys the in-plane order in the layers. Continuing the shear for (60 ns) results in sudden reordering of the dodecane molecules in the flow direction and the reduction in the film thickness and shear stress. This formation is not unique and multiple states might result. In some cases only a few layers might align in the flow direction and the rest might orient in a different direction. In some of the simulations molecular orientation is at an angle with the flow direction and still the result is a film with lower friction. This is shown in figure 13 where the film is being sheared at 10^{10} s^{-1} . The molecules in each domain are extended with their axis making a 45° angle with the shear direction. Depending on how the layers form the rheological response is different. We have displayed some of these results in figure 15 where the shear viscosity is plotted against the shear rates for these multiple states. The high friction that has the “mosaic like” structure up until shear rates $< 10^{9.5} \text{ s}^{-1}$ is shown to start the shear thinning at much

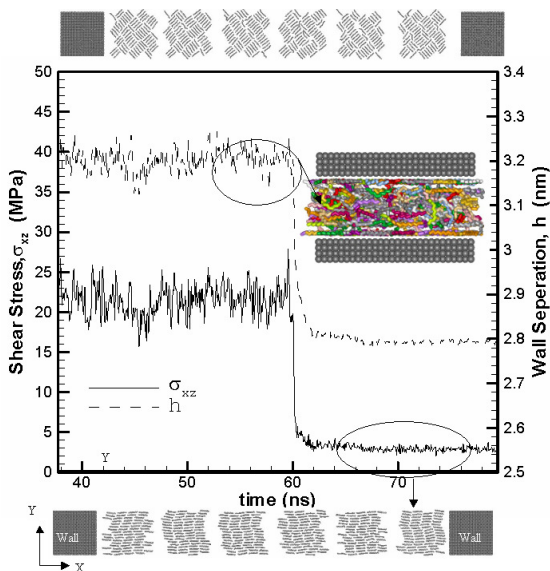


Figure 12: Transition of a 6 layer film of dodecane confined between two model mica walls made of 100 plane of fcc lattice. The equilibration of the film initially produces a highly layered film with tetratic order (shown in figure 7). Applying the shear initially destroys order in the film (shown in the inset) and then film reorders, only this time all lined up in the flow direction. The results is a film whose effective viscosity is even less than that of bulk dodecane. The snapshots at the top and bottom show the molecular orientation in the individual layers. From Jabbarzadeh A, Harrowell P, Tanner R I, Phys.Rev.Lett. 94, 126103, 2005. Copyright (2005) by American Physical Society [106].

lower shear rates not accessible by our simulations. However the experimental results are shown to be catching up with simulation results at lower shear rates. In contrast the low viscosity films behave as Newtonian and only start to show shear thinning at higher shear rates. Significantly, all the low friction films exhibit a Newtonian viscosity lower than that of the bulk dodecane (~ 1.34 mPas). This is significant as these highly ordered films of low friction films remain stable and even at high shear rates do not get disordered. The observed phenomena is very similar to the so called “memory effect” that is seen in “stop-start” shearing experiments [61].

The transition to these low shear viscosity regimes is accompanied by significant slippage. The nature of the slip of course can be quite different depending on the

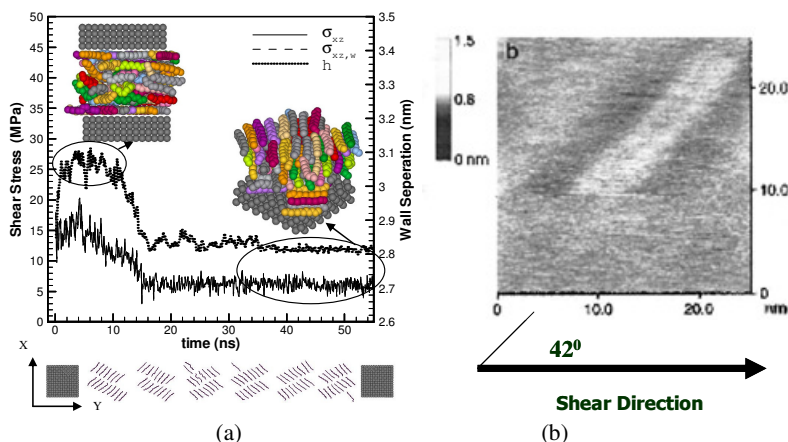


Figure 13: (a) Transition to low friction film in the simulation of dodecane with domains in the layers making a $\sim 45^\circ$ angle with the shear direction. (b) Similar domains a few nanometres wide have been reported in the recent experiments on confined films of n-eicosane ($C_{20}H_{42}$) [82]. Note the shear is applied in the X direction (reprinted figure 3b from Drummond C, Alcantar N, and Israelachvili J, Phys. Rev. E. 66, 011705, (2002). Copyright (2002) by American Physical Society).

molecular orientation of the molecules in the layers. These are shown in figure 14 where we can see the slippage happens more significantly within the film. For the film whose molecules are in all 6 layers aligned in hexagonally packed form the slip happens within the film and it is equally distributed between layers. The mechanism of this low friction film is very similar to what happens for a solid lubricant such as graphite where individual layers slip on top of each other. A similarity can also be drawn with nematic phase liquid crystal films [112]. For the film with 45° alignment, however, there are multiple slip planes both within the film (only one slip plane) and at the dodecane-mica interfaces. Barrat and Bocquet [113] have argued that structural mismatch between a liquid and a solid surface can result in a significant reduction in the interfacial friction and hence enhance wall slip. We are unaware of any results indicating the consequences of this structural mismatch in a thin lubricating film.

The low friction films are distinct from what is perceived as superlubricity where low friction between solid-solid contacts happens due to incommensurability of the two surfaces in contact [66]. Here the main slip happens within the film (particularly in fully aligned films). The internal slippage shown for the film in figure 14b happens due to mismatch of the crystalline bridges that form across the film. We see clearly this mismatch from the molecular orientation snapshot shown at the bottom of figure 13. We

will come back to this mismatch issue in the next section when we discuss the surface effect.

Similar observations of domains with an angle to the shear direction are reported in experiments on slightly longer alkane molecules of n-eicosane ($C_{20}H_{42}$) by Drummond et al [82]. Traditionally it is believed, mainly based on the computer simulations of

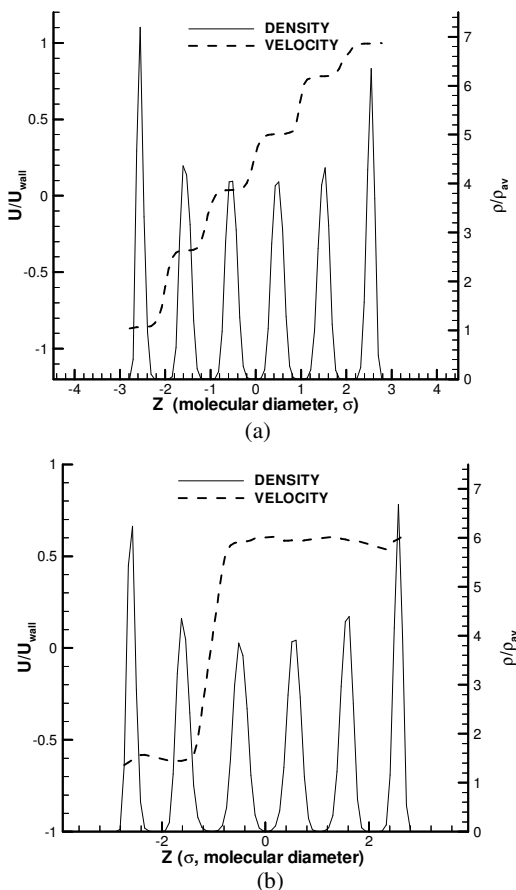


Figure 14: Density and velocity (in shear direction) profiles for the two low friction films shown in (a) figure 12 and (b) figure 13a. The viscosities and densities are normalized respectively by wall velocity and average density of the film.

soft LJ spheres by [64, 114], that solid-like to liquid-like transition is the main route of transition from the static friction regime to the kinetic friction in thin film lubricants. The signature of this event is intermittent “freezing” and “melting” of the confined film manifested by stick-slip behaviour. A steady state kinetic friction regime characterised by smooth sliding is reached when the film is fully melted and can not get back to an ordered “solid like” state. Our simulation results, also suggestions from experiment [82] now suggest that there might another route to kinetic friction and that is through alignment and order within the film. This route leads to a much lower kinetic friction.

The low friction films shown in figure 15 are shown to be in a lower energy state than that of high friction film with a mosaic-like structure [106] suggesting they might be the true equilibrium state of the film and the mosaic-like structures are only metastable states. Recent experiments by Zhu and Granick [84] are thought to be a strong indication of this hypothesis. In that experiment the longer waiting time for equilibrium (by moving the mica surface towards each other slower) resulted in a film with much lower viscosity than that formed by squeezing the film faster.

The results here also explain behaviour observed for very thin films regarding stick-slip, memory effects and transition from stick-slip to smooth kinetic friction regime. Historically many of the previous simulations that captured the stick-slip

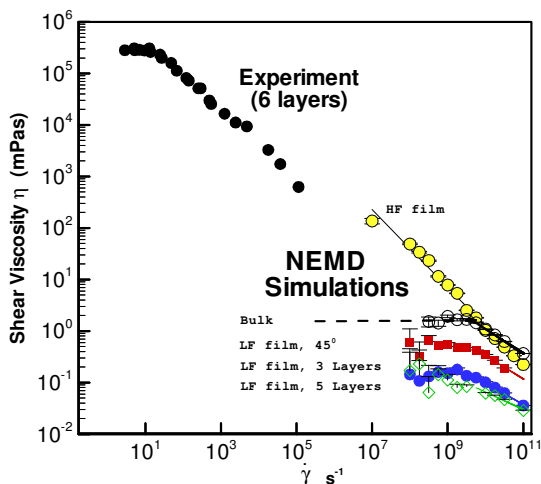


Figure 15: Multiple rheological states of a 6-layer (~2.4 nm) dodecane film confined between atomically smooth model mica walls made of a 100 plane FCC lattice. The experimental results of Hu et al [71] are also plotted here.

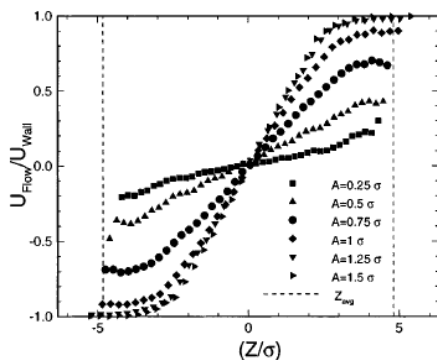
behaviour involved setting up simulations that had a similar setting to experiments with the surfaces attached to springs and a fictitious mass to reproduce the experimental findings. However we have been able to get atomic scale stick-slip behaviour out of our simulations that are basically two solid walls with a sandwiched layer of lubricant film.

3.2.5 The role of surfaces in rheological response of the film

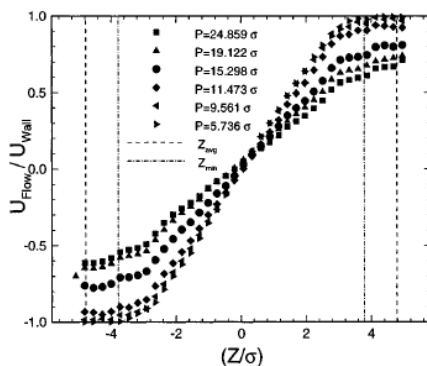
The structure of the confined film generally dictates its mechanical properties. Due to the small scale of the system the confining surfaces naturally have a significant effect on the film structure and its ultimate properties. There have been systematic studies on the effect of surface energy and density on the film properties [88, 104]. The increased density of the walls makes the layers immediately next to the walls denser. The walls with higher surface energy increase the adsorption level of the molecules onto the wall and naturally affect their order. Those in turn have profound effects on how the film interacts with the wall and the momentum transfer and boundary conditions are affected in turn.

Despite these works the effect of surface morphology and topology in atomic scales is less studied. Limited existing research on the effect of surface roughness [105, 115] indicates that even roughness at atomic scale has a profound effect on the film layering, order, boundary condition and rheological response. Using a simple sinusoidal wall with model alkane films it has been shown that the wall slip increases with wall roughness period and the size of the molecules. The wall slip decreases with increased wall roughness amplitude. [See figure 16]. In simulations with atomically rough and smooth gold surfaces Gao et al [115] have shown that a four-layer film of hexadecane behaves quite differently depending on the surface used. They have observed the shear stress with the smooth wall is much lower than that is measured for films confined between the rough surfaces. The main reason for this is due to significant surface slip that occurs with smooth flat surfaces. The average roughness of the roughened wall is only few times the size of ethyl segments that constitutes the hexadecane chain, yet the effect is profound. This is shown in figure 17.

Much less work has been done on the effect of the surfaces atomic structure and order, relative commensurability, crystallographic direction, shear direction and relative position of the two confining surfaces. Even less attention has been paid so far to the structure of the surface in terms of atomic arrangement and order. We recently conducted studies [116] on the effect of wall atomic order on the properties of the confined film in static and dynamic situations. We used an amorphous wall which was basically a bcc wall that was melted at very high temperature and then the amorphous state was frozen and used as a surface. The produced wall was very smooth at the atomic levels having a roughness of $(0.06 \text{ nm}) 0.14 \sigma$ when measured using a method described in [115]. The same method gave the roughness of a FCC wall shown in figure 7 to be 0.016 nm (0.04σ). This roughness was much smaller than that was used in the Gao et al [115] work. However to bring the level of roughness of the amorphous wall to the same level as the crystalline wall (to isolate the effect of the amorphousness of the wall) we used a very short range barrier wall [104] that shaved off some of the



(a)



(b)

Figure 16: The effect of (a) roughness period and (b) roughness amplitude on the velocity profiles for average film thickness of 3.9 nm (9.637σ). The dashed line shows the average film thickness position [105]. From Jabbarzadeh A, Atkinson J D, and Tanner R I, Phys. Rev. E, 61, 690, 2000. Copyright (2000) by American Physical Society.

troughs on the surface to reduce the effective roughness. Scanning through the modified amorphous wall this time gave the roughness value to be (0.04σ) similar to that of the FCC wall.

Equilibrating the amorphous wall with no roughness modification resulted in a film with no structural order. The modified amorphous surface with roughness equal to that of mica produced a film with a sharper layering effect and in-plane ordering. A

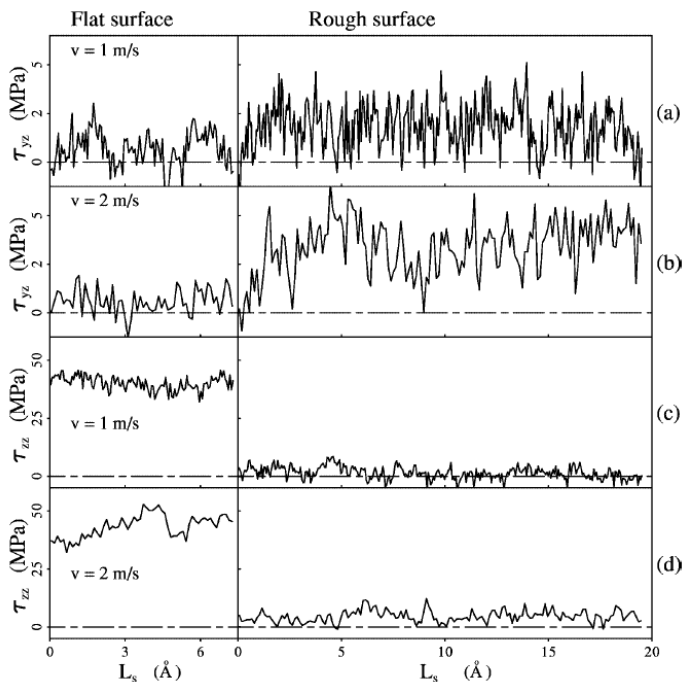


Figure 17: Molecular dynamics simulation results for normal and shear stresses for a 4-layer film confined between flat (left panels) and rough (right panels) surfaces undergoing shear, v is the velocity of the moving wall and here it is shown for $v = 1$ m/s ($\dot{\gamma} \sim 10^9$ s $^{-1}$) and $v = 2$ m/s ($\dot{\gamma} \sim 2 \times 10^9$ s $^{-1}$) [115]. (Reprinted from Gao J, Luedtke W and Landman U, “Structures, solvation forces and shear of molecular films in a rough nano-confinement”, Tribology Lett., 9 (2000) 3-13.)

single patch of molecules aligned parallel to each other on the surfaces led to the formation of a single crystalline bridge across the film. However in this case, unlike those formed with FCC surfaces, the orientation direction of the axes of the molecules in the bridge did not have any preferential direction and was random. The rest of the film remained disordered. Snapshots of the films that were produced are shown in figure 18.

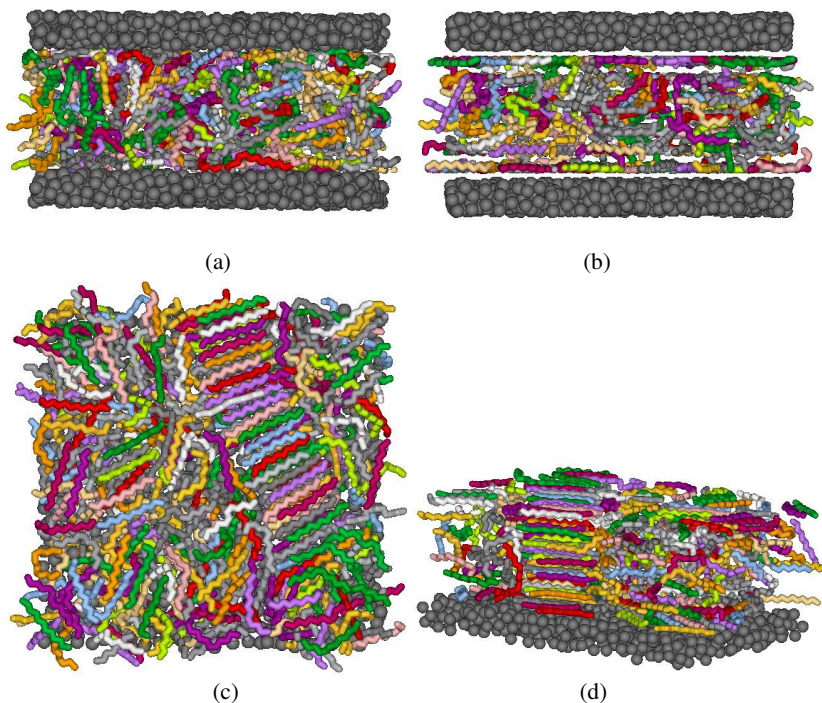


Figure 18: Snapshots of dodecane films confined between the (a) unmodified amorphous walls, (b) modified amorphous film with roughness equal to that of a model mica wall. (c) and (d) the same system as (b), from side and top views respectively. Note the formation of a small patch of ordered phase that has led to the formation of single crystalline bridge. The films have been equilibrated for significant times of 47 ns (10 million time steps) and no further change in the structure was observed.

When these films were subjected to shear there were a marked differences between the rheological properties of the film in between the model mica surface with FCC structure and those between the amorphous walls. The shear response of these films is shown in figure 19. We can see in this figure that the high viscosity state of the mosaic-like structure of the film confined between the FCC walls gives way to a film with low viscosity which is only marginally higher than that of the bulk dodecane. The modified “smooth amorphous” walls on the other hand produce a film with more

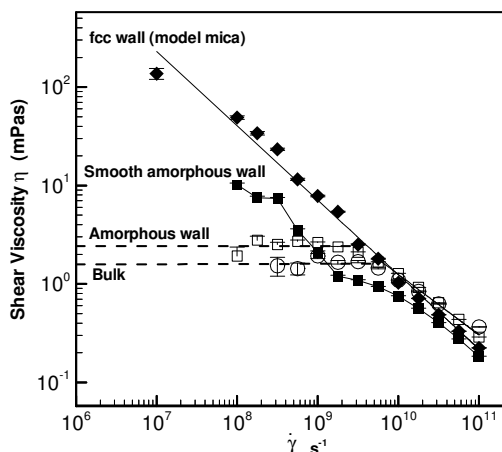


Figure 19: Shear viscosity vs. shear rate for a nominal 6-layer film of dodecane. Note the marked difference in rheological response with different walls. For the amorphous wall the density is the same as the fluid ($1.95 \sigma^{-3}$). Using a slightly lower density close to that of FCC wall ($1.85 \sigma^{-3}$) densities provided similar results. The marked sudden drop of shear viscosity for the film confined between smooth amorphous walls corresponds to the destruction of crystalline bridges that contribute to increased viscosity.

enhanced viscosity due to the presence of the crystalline bridges that form only randomly. This higher viscosity film though drops to a lower viscosity as soon as the bridges are destroyed. At this stage there is a sudden reduction in the viscosity that corresponds to shear induced destruction of the bridges at shear rates $> 10^{8.5} \text{ s}^{-1}$. One should bear in mind that this artificially built modified “smooth amorphous” wall used here to isolate the effect of the amorphousness and wash out the roughness effect from our results. The results show the formation of in-plane order requires an atomic smoothness where the average roughness has to be less than one tenth of the probing segments diameters. At the same film thickness of roughly 6-7 molecular diameters the smooth wall will only produce randomly oriented bridges that will be destroyed under shear more easily. Tightly knit mosaic-like structure, formed with the crystalline surface, clearly results in a higher viscosity. At this thickness we can see even the “smooth amorphous” wall can not match the viscosity enhancement that is produced by a crystalline wall. However we can not rule out stronger in-plane order at thinner films with a “smooth amorphous” wall. Although even in that case we expect the direction of molecules in the formed domains to be rather random.

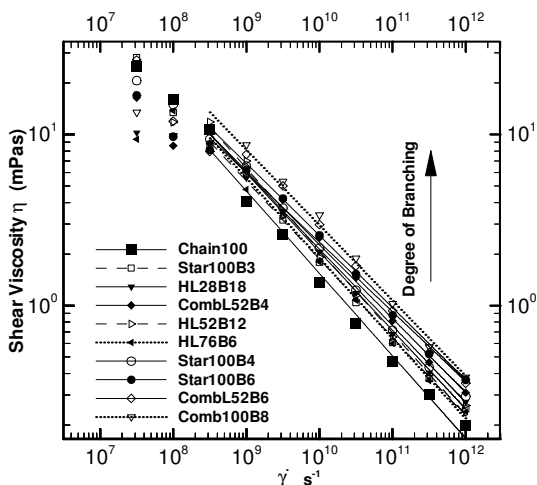


Figure 20: Shear viscosity vs. the shear rate for linear, star, H and comb shaped isomers of $C_{100}H_{202}$ model polyethylene. Degree of branching is defined as the number of branching points per 100 carbon atoms on the effective length (the longest route between the free ends of the molecule).

We are currently looking on the effect of crystalline surface commensurability on the response of these films to shear and we find these subtle details have tremendous effect on the film response and apparent rheological response similar to those reported by Yoshizawa et al [63].

3.2.6 The role of molecular structures on the film properties

The molecular structure of the liquids dictates the physical and rheological properties of the liquids. Nowadays development of new synthesizing methods has made it possible to produce novel new materials. Molecular dynamics can be used as a valuable tool to study the properties of the materials from their molecular structure. The detailed control over the structure gives the ability to study the properties of materials even before they are synthesized in the laboratory. Recent simulations of the long C_{100} polyethylene [103, 117] and dendrimers [118] can be mentioned as a growing trend in this direction. A systematic study of the effect of branching on linear, star, H and comb shaped C_{100} molecules shows consistent increase of shear viscosity with the degree of branching for bulk polymers (see figure 20). The effect of degree of branching on the rheological properties of confined alkane chains was studied by MD simulations [102] and similar conclusions were drawn for the viscosity. It is shown

that the degree of branching also affects the boundary conditions with larger slip experienced as the degree of branching is increased. These simulations however have been done with lower surface energies and for relatively thick films where “solid-like” transitions are not expected. More detailed simulations for mica-alkane systems with thinner films where “solid-like” transitions might happen could also be beneficial. Studying branched molecules could shed light on the effect of molecular structure on the formation of solid-like domains and hence on the response to shear before and after phase transitions. The experiments on various types of molecules report similar exotic behaviour; however the phase transition could be different depending on the architecture of the molecules. Such investigations could lead to detection of novel new structures that could have rheological properties of interest in industrial applications.

4. CONCLUSIONS AND THE FUTURE

In this article we have concentrated on the prediction of rheological properties under shear using molecular dynamics simulation computations. These methods are appropriate in looking at phenomena where the channel size and/or the surface roughness approach molecular size. In this case the major finding has been that when the channel width is reduced below about seven molecular diameters or sizes comparable to the size or radius of gyration of the confined molecules a significant increase in the viscosity is seen. However this transition to high viscosity depends on many factors such as the surface energy, wall smoothness and crystalline order. Depending on these the confined fluid may exhibit multiple rheological states. It may retain its fluidity and show enhanced viscosity only a few times that of the bulk due to geometrical constraints. It might change phase to highly ordered structures and depending on the structures formed the rheological response could range from an extremely high viscosity 6-7 orders of magnitude larger than the bulk or films with viscosity even lower than the bulk. Some of the dodecane films that we have simulated change to ordered phases usually only seen with liquid crystals. The findings of these simulations greatly assist us in understanding the behaviour of thin lubricating films. In addition when the detailed studies of the fluid/surface interactions are made, one sees that the wall slip is common, and that the details and patterns of the surface roughness can influence the rheological response significantly. Areas of order (solid-like) and disorder (liquid-like) can be simultaneously present. In some cases spectacularly low friction is found (figure 15), which may have practical applications. Experimental and simulation work suggests thin film lubricant properties depend on many factors and every little detail counts in their rheological response. The film thickness and molecular structure; surface energy, topology, structure, crystallographic direction and relative orientation are among many important parameters that affect the results. The response of the film is so entangled with these parameters that confined thin film lubricants should be considered as a composite system whose response are mainly driven from combined film-surface details. This approach suggests a universal generic description of film rheology is often inaccurate at best and depending on the details, multiple rheological states might exist even for the same fluid-surface system. Most of the work has been done with straight-chains alkanes (C_nH_{2n+2}) with n up to $O(10^2)$, but it has been possible to extend the work to more complex molecules

containing for example short or long chain branches and rings of atoms. Since the microstructure is precisely specified, one is able to be certain about the effect of molecular architecture on rheology including the first and second normal stress differences (see section 3.2.2).

Whilst the bulk of this review is confined to shearing it is possible to consider elongational flows e.g. [7], using these methods. More complex geometries can also be approached (e. g. figure 4) including the quest for detailed knowledge about the state of flow near sharp corners. Crystallization with flow can also be simulated, and the effects of chemical reactions under flow can also be considered in the future.

Nonetheless, despite these successes, MD methods need caution in their use. Typically, except for using Green-Kubo [6] methods, the method works best at high shear rates ($>10^7 \text{ s}^{-1}$). Below this signal/noise ratio in the computations is too small to give reliable results. Clearly this is an area where the improvements would be welcome. Another source of much dispute among the practitioners is the question of how thermostating should be done for “isothermal” problems. We have described some well-tried methods above, but especially at very high shear rates, there are still many debates. We believe MD will increasingly be a useful tool in resolution of nano-technology problems in the near future.

ACKNOWLEDGEMENTS

This work was supported by a Discovery Grant from the Australian Research Council. We also thank the Australian Centre of Advanced Computing and Communications and also the Australian Partnership For Advanced Computing National Facility for the generous time allocated for computing.

REFERENCES

1. Laplace, P S, “Philosophical Essay on Probabilities”, (translation) Dover, New York, (1951).
2. Haile, J M, “Molecular dynamics simulation, elementary methods”, John Wiley & Sons New York, (1992).
3. Allen, M P and Tildesley, D J, “Computer simulation of liquids”, Clarendon Press Oxford, (1987).
4. Rapaport, D C, “The Art of Molecular Dynamics Simulation”, Cambridge University Press, (1995).
5. Evans, D J and Morriss, G P, “Statistical Mechanics of Nonequilibrium Liquids”, Academic Press, (1990).
6. Green, M S, “Markoff random processes and the statistical mechanics of time-dependent phenomena: 2. Irreversible processes in fluids”, *J. Chem Phys*, 22 (1954) 398-413; Kubo, R, “Statistical-mechanical theory of irreversible

- processes. I. General theory and simple applications to magnetic and conduction problems", *J. Phys. Soc. Japan*, 12 (1957) 570-586.
7. Matin, M L, Davis, P J and Todd, B D, "Comparison of planar shear flow and planar elongational flow for systems of small molecules", *J. Chem. Phys.*, 113 (2000) 9122-9131.
 8. Metropolis, N, Rosenbluth, A W, Rosenbluth, M N, Teller, A H and Teller, E, "Equation of state calculations by fast computing machines", *J. Chem. Phys.*, 21 (1953) 1087-1092.
 9. Wood, W W and Parker, F R, "Monte Carlo equation of state of molecules interacting with the Lennard-Jones potential. I. A supercritical isothermal at about twice the critical temperature", *J. Chem. Phys.*, 27 (1957) 720-733.
 10. Alder, B J and Wainwright, T E, "Phase transition for a hard sphere system", *J. Chem. Phys.*, 27 (1957) 1208-1209.
 11. Rahman, A, "Correlations in the motion of atoms in liquid argon", *Phys. Rev. A*, 136 (1964) 405-411.
 12. Harp, G D and Berne, B J "Linear and angular momentum autocorrelation functions in diatomic liquids", *J. Chem. Phys.*, 49 (1968) 1249-1254.
 13. Rahman, A and Stillinger, F H "Molecular dynamics study of liquid water", *J. Chem. Phys.*, 55 (1971) 3336-3359.
 14. Barojas, J, Levesque, D and Quentrec, B, "Simulation of diatomic homonuclear liquids", *Phys. Rev. A*, 7 (1973) 1092-1105.
 15. Ryckaert, J P and Bellemans, A, "Molecular dynamics of liquid n-butane near its boiling point", *Chem. Phys. Lett.*, 30 (1975) 123-125.
 16. McCammon, J A, Gelin, B R and Karplus, M, "Dynamics of folded proteins", *Nature*, 267 (1977) 585-590.
 17. Lees, A W and Edwards, S F, "The computer study of transport process under extreme conditions", *J. Phys. C*, 5 (1972) 1921-1929.
 18. Ashurst, T and Hoover, W G, "Dense fluid shear viscosity via non-equilibrium molecular dynamics", *Phys. Rev. A*, 11 (1975) 658-678.
 19. Evans, D J, "The frequency dependent shear viscosity of methane", *Mol. Phys.* 37, (1979) 1745-1754
 20. Heyes, D M, Evans, D J and Morriss, G P, "Nonequilibrium molecular dynamics study of shear flow in soft disks", *J. Chem. Phys.*, 85 (1985) 4760-4765.
 21. Evans, D J and Morriss, G P, "The isothermal/isobaric molecular dynamics ensemble", *Phys. Lett. A*, 98 (1983) 433-436.
 22. Evans, D J and Morriss, G P, "Nonlinear-response theory for steady planar Couette flow", *Phys. Rev. A*, 30 (1984) 1528-1530.

23. Evans, D J and Morriss, G P, "Isothermal response theory' *Molec. Phys.*, 54 (1985) 629-636.
24. Evans, D J, "Rheological properties of simple fluids by computer simulation", *Phy. Rev. A*, 23 (1981) 1988-1997.
25. Hood, L M, Evans, D J and Hanley, H J M, "Properties of a soft-sphere liquid from non-Newtonian molecular dynamics", *J. Stat. Phys.*, 57 (1989) 729-749.
26. Evans, D J "Non-equilibrium molecular dynamics study of the rheological properties of diatomic liquids", *Molec. Phys.*, 42 (1981) 1355-1365.
27. Rudisill, J W and Cummings, P T, "The contribution of internal degrees of freedom to the non-Newtonian rheology of polymer fluids", *Rheologica Acta*, 30 (1991) 33-43.
28. Rudisill, J W and Cummings, P T, "Non-equilibrium molecular dynamics approach to the rheology of model polymer fluids", *Fluid Phase Equilibria*, 88 (1993) 99-113.
29. Hess, S, "Rheological properties via nonequilibrium molecular dynamics: from simple towards polymeric liquids", *J. Non-Newtonian Fluid Mech.*, 23 (1987) 305-319.
30. Edberg, R, Evans, D J and Morriss, G P, "Constrained molecular dynamics: simulation of liquid alkanes with a new algorithm", *J. Chem. Phys.*, 84 (1986) 6933-6939.
31. Edberg, R, Evans, D J and Morriss, G P, "On the nonlinear Born effect", *Molec. Phys.*, 62 (1987) 1357-1369.
32. Edberg, R, Evans, D J and Morriss, G P, "Rheology of n-alkanes by nonequilibrium molecular dynamics", *J. Chem. Phys.*, 86 (1987) 4555-4570.
33. Davis, P J, Evans, D J and Morriss, G P, "Computer simulation study of the comparative rheology of branched and linear alkanes", *J. Chem. Phys.*, 97 (1992) 616-627.
34. Verlet, L, "Computer experiments on classical fluids. I. Thermodynamical properties of Lennard-Jones molecules", *Phys. Rev.*, 159 (1967) 98-103.
35. Gear, W C, "The numerical integration of ordinary differential equations of various orders", Report ANL 7126, Argonne National Laboratory, (1966).
36. Gear, W C, "Numerical initial value problems in ordinary differential equations", Prentice-Hall, Englewood Cliffs, NJ, (1971).
37. Heyes, D M, "The liquid state Applications of molecular simulations", John Wiley UK, (1998).
38. McQuarrie, D A, "Statistical mechanics", Harper and Row, New York, (1976).

39. Lennard-Jones, J E, "The determination of molecular fields. I. From the variation of the viscosity of a gas", *Proc. Roy. Soc. (Lond.)*, 106A (1924) 441-448.
40. Quentrec, B and Brot, C, "New methods for searching for neighbors in molecular dynamics computations", *J. Comput. Phys.*, 13, 430-432 (1975).
41. Irving, J H and Kirkwood, J G, "The statistical mechanical theory of transport process. IV. The equations of hydrodynamics", *J. Chem. Phys.*, 18, 817-829 (1950).
42. Bitsanis, I, Magda, J J, Tirrell, M and Davis, H T, "Molecular dynamics of flow in micropores", *J. Chem. Phys.*, 87, 1733-1750 (1987).
43. Todd, B D, Evans, D J and Daivis, P J, "Pressure tensor for inhomogeneous fluids", *Phys. Rev. E*, 52, 1627-1638 (1995).
44. Evans, D J and Morriss, G P, "Shear thickening and turbulence in simple fluids", *Phy. Rev. Lett.*, 56, 2172-2175 (1986).
45. Liem, S Y, Brown, D and Clarke, J H R, "Investigation of the homogeneous-shear nonequilibrium-molecular-dynamics method", *Phys. Rev. A*, 45 (1992) 3706-3713.
46. Travis, K P, Daivis, P and Evans, D J, "Thermostats for molecular fluids undergoing shear flow: Application to liquid chlorine", *J. Chem. Phys.*, 103 (1995) 10638-10651.
47. Gao, J, Luedtke, W D and Landman, U, "Structure and solvation forces in confined films: Linear and branched alkanes", *J. Chem. Phys.*, 106, (1997) 4309-4318.
48. Borzsak, I, Cummings, P T and Evans, D J, "Shear viscosity of a simple fluid over a wide range of strain rates", *Mol. Phys.* 100 (2002) 2735-2738.
49. Arya, G, Maginn, E J and Chang, H, "Efficient viscosity estimation from molecular dynamics simulation via momentum impulse relaxation", *J. Chem. Phys.* 113 (2000) 2079-2087.
50. Bailey, A I and Courtney-Pratt, J S, "The area of real contact and the shear strength of monomolecular layers of a boundary lubricant", *Proc. Roy. Soc.*, A227 (1955) 500-515.
51. Israelachvili J N, and Tabor D, "The shear properties of molecular films", *Wear*, 24 (1973) 386-390.
52. Chan, D Y C and Horn, R G, "The drainage of thin liquid films between solid surfaces", *J. Chem. Phys.*, 83, 5311-5323 (1985).
53. Israelachvili, J N, "Measurements of the viscosity of thin fluid films between two surfaces with and without adsorbed polymers", *Colloid & Polymer Sci.*, 264 (1986) 1060-1065.

54. Israelachvili, J N, "Direct measurement of interactions and viscosity of crude oils in thin films between model clay surfaces", *Colloid & Interface Sci.*, 119 (1987) 194-202.
55. Israelachvili, J N, McGuiggan, P M and Homola, A M, "Dynamic properties of molecularly thin liquid films", *Science*, 240 (1988) 189-190.
56. Israelachvili, J N, "Measurement of the viscosity of liquids in very thin films", *Colloid & Interface Sci.*, 110 (1986) 263-270.
57. Gee, M L, McGuiggan, P M and Israelachvili, J N, "Liquid to solid like transitions of molecularly thin films under shear", *J. Chem. Phys.*, 93 (1990) 1895-1906.
58. Christenson, H K, Gruen, D W R, Horn, G, and Israelachvili, J N, "Structuring in liquid alkanes between solid surfaces: Force measurement and mean field theory", *J. Chem. Phys.*, 87 (1987) 1834-1841.
59. Horn, G and Israelachvili, J N, "Direct measurement of structural forces between two surfaces in a nonpolar liquid", *J. Chem. Phys.*, 75 (1981) 1400-1411.
60. Yoshizawa, H and Israelachvili, J, "Fundamental mechanisms of interfacial friction. 1. Relation between adhesion and friction" *J. Phys Chem*, 97 (1993) 4128-4140
61. Yoshizawa, H and Israelachvili, J, "Fundamental Mechanisms of Interfacial Friction. 2. Stick-Slip Friction of Spherical and Chain Molecules" *J Phys Chem*, 97 (1993) 11300-11313.
62. Yoshizawa, H, McGuiggan, P and Israelachvili, J, "Identification of a second dynamic state during stick-slip motion", *Science*, 259 (1993) 1305-1308.
63. Yoshizawa, H and Israelachvili, J, "Relation between adhesion and friction forces across thin films", *Thin Solid Films*, 246 (1994) 71-76.
64. Thompson, P A and Robbins, M O, "Origin of Stick-Slip Motion in Boundary Lubrication" *Science*, 250 (1990) 792-794.
65. Aranson, I S, Tsimring, S and Vinokur, V M, "Stick-slip friction and nucleation dynamics of ultrathin liquid films", *Physical Review B*, 65 (2002) 125402-1/7.
66. Hirano, M, and Shinjo, K and Kaneko, R, "Anisotropy of frictional forces in muscovite mica", *Phys. Rev. Lett.* 67 (1991) 2642-2646.
67. Ruths, M and Granick, S, "Influence of Alignment of Crystalline Confining Surfaces on Static Forces and Shear in a Liquid Crystal, 4*c*-n-Pentyl-4-cyanobiphenyl", *Langmuir* 16 (2000) 8368-8376.
68. Van Alsten, J and Granick, S, "Molecular tribometry of ultrathin liquid films", *Phys. Rev. Lett.*, 61 (1988) 2570-2573.
69. Van Alsten, J and Granick, S, "The origin of static friction in ultrathin liquid films", *Langmuir*, 6 (1990) 876-880.

70. Van Alsten, J and Granick, S, "Shear rheology in a confined geometry: polysiloxane melts", *Macromolecules*, 23 (1990) 4856-4862.
71. Hu, H W, Carson, G A and Granick, S, "Relaxation time of confined liquids under shear", *Phy. Rev. Lett.*, 66 (1991) 2758-2761.
72. Van Alsten, J and Granick, S, "Tribology studies using atomically smooth surfaces", *Tribol. Trans.*, 33 (1990) 436-446.
73. Granick, S and Hu, H W, "Nanorheology of confined polymer melts. 1. Linear shear response at strongly adsorbing surfaces", *Langmuir*, 10 (1994) 3857-3866.
74. Granick, S, Hu, H W and Carson, A, "Nanorheology of confined polymer melts. 2. Nonlinear shear response at strongly adsorbing surfaces", *Langmuir*, 10 (1994) 3867-3873.
75. Peanasky, J, Cai, L L and Granick, S, "Nanorheology of confined polymer melts. 3. Weakly adsorbing surfaces", *Langmuir*, 10 (1994) 3874-3879.
76. Luengo, G, Israelachvili, J and Granick, S, "Generalized effects in confined fluids: New friction map for boundary lubrication", *Wear* 200 (1996) 328-335.
77. Jabbarzadeh, A, Atkinson, J D and Tanner, R I, "Nanorheology of molecularly thin films of n-hexadecane in Couette shear flow by molecular dynamics simulation", *J. Non-New. Fluid Mech.*, 77 (1998) 53-78.
78. Luengo, G, Schmitt, F, Hill, R and, Israelachvili, J, "Thin Film Rheology and Tribology of Confined Polymer Melts: Contrasts with Bulk Properties", *Macromolecules*, 30 (1997) 2482-2494.
79. Drummond, C and Israelachvili, J," Dynamic phase transitions in confined lubricant fluids under shear", *Phys. Rev. E*, 63 (2001) 041506-1/11.
80. Drummond, C and Israelachvili, J, "Dynamic behavior of confined branched hydrocarbon lubricant fluids under shear", *Macromolecules*, 33 (2000) 4910-4920.
81. Golan, Y, Martin-Herranz, A, Li, Y, Safinya, C R and Israelachvili, J, "Direct observation of shear-induced orientational phase coexistence in a lyotropic system using a modified x-ray surface forces apparatus", *Phys Rev. Lett*, 86 (2001) 1263-1266.
82. Drummond, C, Alcantar, N and Israelachvili, J, "Shear alignment of confined hydrocarbon liquid films", *Phys. Rev. E*. 66 (2002) 011705-1/6.
83. Zhu, Y and Granick, S, "Reassessment of solidification in fluids confined between mica sheets" *Langmuir* 19 (2003) 8148-8251
84. Zhu, Y and Granick, S," Superlubricity: A paradox about confined fluids resolved" *Phys. Rev. Lett.* 93 (2004) 096101-1/4.

85. Klein, J and Kumacheva, E, "Simple liquids confined to molecularly thin layers. I. Confinement-induced liquid-to-solid phase transitions" *J. Chem Phys.* 108 (1999) 6996-7009.
86. Granick, S, "Motion and relaxation of confined liquids" *Science*, 253 (1991) 1374-1379.
87. Thompson, P A and Grest, G S, "Phase transitions and universal dynamics in confined films", *Phy. Rev. Lett.*, 68 (1992) 3448-3451.
88. Thompson, P A and Robbins, M O "Shear flow near solids: Epitaxial order and flow boundary conditions", *Phys. Rev. A*, 41 (1990) 6830-6837.
89. Bitsanis, I, Somers, S A, Davis, H T and Tirrell, M, "Microscopic dynamics of flow in molecularly narrow pores", *J. Chem. Phys.*, 93 (1990) 3427-3431.
90. Magda, J J, Tirrell, M and Davis, H T, "Molecular dynamics of narrow, liquid-filled pores", *J. Chem. Phys.*, 83 (1985) 1888-1901
91. Bitsanis, I, Vanderlick, T K, Tirrell, M and Davis, H T, "A tractable molecular theory of flow in strongly inhomogeneous fluids", *J. Chem. Phys.*, 89 (1988) 3152-3162.
92. Barsky, S and Robbins, M O, "Bulk and interfacial shear thinning of immiscible polymers", *Phys. Rev. E*, 65 (2002) 0218081-7.
93. Lupkowski, M and van Swol, F, "Computer simulation of fluids interacting with fluctuating walls", *J. Chem. Phys.*, 93 (1990) 737-745.
94. Lupkowski, M and van Swol, F, "Ultrathin films under shear", *J. Chem. Phys.*, 95 (1991) 1995-1998.
95. Israelachvili, J N, "Intermolecular and surface forces", 2nd ed. Academic Press, San Diego (1992).
96. Schoen, M, Cushman, J H and Diestler, D J, "Fluids in micropores. I. Structure of a simple classical fluid in a slit-pore", *J. Chem. Phys.*, 87 (1987) 5464-5476.
97. Schoen, M, Cushman, J H, Diestler, D J and Rhykerd, C L Jr, "Fluids in micropores. II. Self-diffusion in a simple classical fluid in a slit pore", *J. Chem. Phys.*, 88 (1988) 1394-1406.
98. Heinbuch, U and Fischer, J, "Liquid flow in pores: no-slip, or multilayer sticking", *Phys. Rev. A*, 40 (1989) 1144-1146.
99. Bitsanis, I and Hadziioannou, G, "Molecular dynamics simulation of the structure and dynamics of confined polymer melts", *J. Chem. Phys.*, 92 (1990) 3827-3847.
100. Bitsanis, I and Pan, C, "The origin of the 'glassy' dynamics at solid-oligomer interfaces", *J. Chem. Phys.*, 99 (1993) 5520-5527.

101. Manias, E, Hadzioannou, G, Bitsanis, I and Ten Brinke, G, ““Stick and slip behaviour of confined oligomer melts under shear. A molecular-dynamics study”, *Europhys. Lett.*, 24 (1993) 99-104.
102. Jabbarzadeh, A, Atkinson, J D and Tanner, R I, “The effect of branching on slip and rheological properties of lubricants in molecular dynamics simulation of Couette shear flow” *Tribology International*, 35 (2002) 35–46.
103. Jabbarzadeh, A, Atkinson, J D and Tanner, R I, “The effect of molecular shape on rheological properties in molecular dynamics simulation of star, H, comb and linear shape polymer melts” *Macromol. ,* 36 (2003) 5020-5031.
104. Jabbarzadeh, A, Atkinson, J D and Tanner, R I, “Wall slip in the molecular dynamics simulation of thin films of hexadecane” *J. Chem. Phys.*, 110 (1999) 2612-2620.
105. Jabbarzadeh, A, Atkinson, J D and Tanner, R I, “The effect of the wall roughness on slip and rheological properties of hexadecane in molecular dynamics simulation of Couette shear flow between two sinusoidal walls”, *Phys. Rev. E*, 61 (2000) 690-699.
106. Jabbarzadeh, A, Harrowell, P and Tanner, R I, “Very low friction state of a dodecane film confined between mica surfaces”, *Phys.Rev.Lett.* 94 (2005) 126103-1/4.
107. Cui, S T, Cummings, P T and Cochran, H D, “Molecular simulation of the transition from liquidlike to solidlike behaviour in complex fluids confined to nanoscale gaps” *J. Chem. Phys.*, 114 (2001) 7189-7195.
108. Cui, S T, Cummings, P T and Cochran H D, “Structural transition and solid-like behaviour of alkane films confined in nano-spacing”, *Fluid Phase Equil.*, 183-184 (2001) 381-387.
109. Cui, S T, McCabe, C, Cummings, P T and Cochran, H D, “Molecular dynamics study of the nano-rheology of n-dodecane confined between planar surfaces”, *J. Chem. Phys.* 118 (2003) 8941-8944
110. Jabbarzadeh, A, Harrowell, P and Tanner, R I, “Crystal bridge formation marks the transition to rigidity in a thin lubrication film”, *Phys Rev Lett.* 96, 206102 (2006).
111. Frenkel, D and Eppenga, R, “Evidence of algebraic orientational order in a two-dimensional hard-core nematic”, *Phys Rev A.*, 31 (1985) 1776-1787.
112. Safinya, C R, Sirota, E B and Plano, R J, “Nematic To Smectic-A Phase-Transition Under Shear-Flow - A Nonequilibrium Synchrotron X-Ray Study”, *Phys. Rev. Lett.* 66 (1991) 1986-1989.
113. Barrat, J L and Bocquet, L, “Influence of wetting properties on hydrodynamic boundary conditions at a fluid/solid interface” *Faraday Disc.* **112**, 119-127 (1999)

114. Stevens, M and Robbins, M O, "Simulation of shear induced melting and ordering", *Phys Rev. E*, 48 (1995) 3778-3792.
115. Gao, J, Luedtke, W and Landman, U, "Structures, solvation forces and shear of molecular films in a rough nano-confinement", *Tribology Lett.*, 9 (2000) 3-13.
116. Jabbarzadeh, A, Harrowell, P and Tanner, R I, "Low friction lubrication between amorphous walls: unravelling the contributions of surface roughness and in-plane disorder", *J Chem Phys.* (submitted).
117. Karayiannis, N C and Mavrantzas, V G, "Hierarchical Modeling of the Dynamics of Polymers with a Nonlinear Molecular Architecture: Calculation of Branch Point Friction and Chain Reptation Time of H-Shaped Polyethylene Melts from Long Molecular Dynamics Simulations", *Macromol.*, 38 (2005) 8583-8596.
118. Bosko, J T, Todd, B D and Sadus, R J, "Molecular simulation of dendrimers and their mixtures under shear: Comparison of isothermal-isobaric, NPT and isothermal-isochoric, NVT ensemble systems", *J. Chem Phys.*, 123 (2005) 034905/1-8.